The benthic toxic dinoflagellate Ostreopsis cf. ovata in the NW Mediterranean Sea: Relationship between sea surface temperature and bloom phenology

K. Drouet, C. Jauzein, S. Gasparini, A-S Pavaux, E. Berdalet, S. Marro, V. Davenet-Sbirrazuoli, R. Siano, R. Lemée

The benthic toxic dinoflagellate *Ostreopsis* cf. *ovata* in the NW Mediterranean Sea: Relationship between sea surface temperature and bloom phenology

Drouet, K.[1,2*], Jauzein, C.[2], Gasparini, S.[1], Pavaux, A-S.[1], Berdalet, E.[3], Marro, S.[1], Davenet-Sbirrazuoli, V.[4], Siano, R.[2] & R. Lemée[1]

[1] Sorbonne Université, CNRS, Laboratoire d'Océanographie de Villefranche (UMR 7093), Villefranche-sur-Mer, FRANCE.

[2] Ifremer, DYNECO Pelagos, F-29280 Plouzané, FRANCE.

[3] Institut de Ciènces del Mar (CSIC), Barcelona, SPAIN.

[4] Direction de l'Environnement, MONACO.

*Corresponding author: kevindrouet83@gmail.com

Highlights:

- Long-term monitoring showed variability in bloom dynamics of *O.* cf. *ovata* in NW Mediterranean Sea.
- A strong positive correlation was observed between spring sea surface temperatures and bloom timing.
- Highest growth rates did not coincide with highest sea surface temperatures.
- Sea surface temperature, nutrient loads, wind regimes and rainfall were the main factors affecting *O.* cf. *ovata* bloom phenology.

Abstract:

Blooms of the toxic benthic dinoflagellate *Ostreopsis* cf. *ovata* can induce ecological and human health issues in certain temperate areas. In order to prevent these negative effects, long-term monitoring studies of *O.* cf. *ovata* blooms have been conducted in several impacted areas to have a comprehensive understanding of bloom dynamics and efficient tools for risk management.

O. cf. *ovata* blooms were monitored every summer (from mid-June to the end of August) on five identified sites in Larvotto beach (Monaco, NW Mediterranean Sea), between 2007 and 2019. This time-series represents one of the largest time-series in the world describing blooms of this species.

Bloom phenological features (timing, duration, maximum cell abundance and growth rate), were found to be highly variable throughout the studied period, and were analyzed as a function of different hydroclimatic parameters, including sea surface temperature (SST). The highest net growth rates were related to temperatures ranging between 21°C and 25°C, and did not coincide with maximal temperature records (27.5°C). Such results suggest that, although global warming possibly influences the expansion of *O.* cf. *ovata* from tropical to temperate waters, the definite impact of temperature on bloom dynamics might be more complex than a simple facilitation factor for algal growth, at least in NW Mediterranean waters.

Furthermore, monthly SST anomalies calculated over this 13-year survey showed a strong positive correlation between spring SST positive anomalies and the bloom starting date, indicating that blooms occurred earlier in the season when spring SSTs were warmer than usual.

Overall results provide tools to modelers and managers who are facing crucial challenges to predict the distribution and phenology of *O.* cf. *ovata* blooms in European coastal waters, moreover in a context of global warming.

Keywords: Benthic HABs; Long-term monitoring; Environmental factors; SST anomalies; Temperature niche; Mediterranean Sea

1. Introduction

Over the past decades, worldwide reports of Harmful Algal Blooms (HABs) have increased and suggest that these events are more intense and frequent in some areas, and may also be extending to new regions (Hallegraeff, 2010; Wells et al., 2020; Hallegraeff et al., 2021). This may be the result of a combination of changing climate factors (Glibert et al., 2014; Kibler et al., 2015; Moore et al., 2008; Tester et al., 2020; Wells & Karlson, 2018), anthropogenic forcing (Anderson et al., 2002; Glibert et al., 2005; Heisler et al., 2008; Fu et al., 2012; Davidson et al., 2014) and the implementation of worldwide monitoring programs which have improved the capacity of HAB detection (Van Dolah, 2000; Anderson et al., 2012; Hallegraeff et al., 2021).

Amongst the organisms causing harmful events, the toxic species belonging to the marine dinoflagellate genus *Ostreopsis* Schmidt (1901) are found from tropical to temperate coastal areas (Faust et al., 1996; Rhodes, 2011). *Ostreopsis* spp. was reported in the Mediterranean Sea for the first time in 1972 in Villefranche-sur-Mer, France (Taylor, 1979), and regularly detected thereafter along the Mediterranean coastlines, with three identified species so far, namely, *Ostreopsis* cf. *ovata* (Fukuyo), *O.* cf. *siamensis* (Schmidt) and *O. fattorussoi* (Accoroni, Romagnoli & Totti). The first bloom of *O.* cf. *ovata*, the most common

69 species in the Mediterranean Sea, was first observed off the Tuscany coast in 1998 (Sansoni et
70 al., 2003) and it has been recurrently blooming since then (e.g. Blanfuné et al., 2015;
71 Accoroni and Totti, 2016). Moreover, *O.* cf. *ovata* blooms have been associated to respiratory
72 problems due to inhalation of aerosols and/or skin irritations after direct contact with the
73 seawater (Barroso García et al., 2008; Brescianini et al., 2006; Durando et al., 2007; Illoul et
74 al., 2012; Pfannkuchen et al., 2012; Tichadou et al., 2010; Tubaro et al., 2011; Vila et al.,
75 2008, 2016). *Ostreopsis* blooms have also been related to mass mortalities of certain
76 invertebrates (Sansoni et al., 2003; Totti et al., 2010) caused either by oxygen limitation due
77 to the excess of microalgal biomass or specific ecotoxic compounds. These noxious effects
78 were attributed to *Ostreopsis* toxins (palytoxin analogues, Ciminiello et al., 2006, 2012,
79 2014), even if this has not been completely proven yet. These toxins have been detected in
80 some fish and invertebrates (Aligizaki et al., 2008; Biré et al., 2013, 2015; Brissard et al.,
81 2014) in the Mediterranean Sea and pose a potential risk of food poisoning in humans too as it
82 was reported in the tropics (Tubaro et al., 2011). Luckily, such problems have not been
83 reported in the Mediterranean Sea yet, but the recurrence of *Ostreopsis* blooms have
84 stimulated its monitoring and intense research in order to prevent human and environmental
85 health risks.

86 A main open question is to identify the environmental drivers directly favoring the
87 recurrency of the *Ostreopsis* blooms, which in the NW Mediterranean Sea, are highly
88 seasonal, occurring during the summer to autumn season (Vila et al., 2001; Mangialajo et al.,
89 2008, 2011; Totti et al., 2010). Likely, a combination of different factors are at play. Moderate
90 hydrodynamics seems to favor *O.* cf. *ovata* cells to remain attached to the substrate (Vila et
91 al., 2001; Barone, 2007; Shears and Ross, 2009; Totti et al., 2010) while rough seas and
92 currents would disperse them. Relatively low wind intensities (2-4 m s^{-1}) were registered
93 concurrently to some blooms in the NW Mediterranean (Vila et al., 2016). The role of nutrient

availability on *Ostreopsis* blooms dynamics is still a matter of debate. For instance, no direct relationship was found between inorganic nutrient concentrations and cell abundances during bloom periods (Vila et al., 2001; Cohu et al., 2011; Pistocchi et al., 2011; Accoroni et al., 2012), although variations of nitrate to phosphate (N:P) ratios may be involved in the onset of the bloom (Accoroni et al., 2015a). These microalgae can assimilate a variety of inorganic and organic compounds, but the complexity of nutritive pathways fueling *Ostreopsis* blooms in the field has still to be characterized, in particular for mixotrophic capability (Accoroni et al., 2017; Jauzein et al., 2017; Lee and Park, 2018). Regarding salinity, laboratory studies showed that *O.* cf. *ovata* grew better under high salinity conditions (Pezzolesi et al., 2012), but salinity preferences would be strain-specific (Tawong et al., 2015). Field observations reported *O.* cf. *ovata* blooms in the 37 and 38 salinity range in the NW Mediterranean Sea (Vila et al., 2001; Mangialajo et al., 2008) and in a wider range (31 – 39) in the Northern Adriatic Sea (Accoroni et al., 2015a) or in the South-Eastern Mediterranean Sea (Abdennadher et al., 2017). Low salinity associated to inflowing freshwater was shown to hinder blooming events (Blanfuné et al., 2015; Carnicer et al., 2015). As *Ostreopsis* spp. cells mainly proliferate in shallow waters (Totti et al., 2010; Cohu and Lemée, 2012), sea depth and substratum play a role in their blooms. High *Ostreopsis* cells abundances are preferentially found on macroalgae with ramified structures in sheltered shallow habitats (Cohu et al., 2013; Accoroni et al., 2015b; Meroni et al., 2018). The seasonality of the macroalgal communities in temperate latitudes, driven by light and temperature intensity, may also be relevant for the *Ostreopsis* blooms to occur.

Indeed, temperature is considered one of the most important environmental factors determining cell biology, growth and reproduction, and it also follows seasonal variations. It has been suggested that *Ostreopsis* spp. growth and bloom development could be favored by relatively high temperatures, as those occurring in summer (Hallegraeff, 2010; Granéli et al.,

2011). In the Atlantic coastline of the Iberian Peninsula, David et al. (2012) found that *Ostreopsis* spp. blooms could be triggered when sea surface temperatures (SSTs) exceeded a certain threshold (namely, 19.5°C) over a long enough period (three months). In the NW Mediterranean Sea, the occurrence of *O.* cf. *ovata* blooms have been reported from 16.8°C to 30°C (Mangialajo et al., 2011; Accoroni and Totti, 2016). Even if major proliferation are usually recorded in mid-summer (July) along the coasts of the Ligurian and Catalan Seas coasts, a second bloom often occurs in autumn in these areas (Mangialajo et al., 2008, 2011; Cohu et al., 2011; Vila et al., 2016). In the Northern Adriatic Sea, blooms even appear rather later in autumn, between September and October (Monti et al., 2007; Totti et al., 2010; Ninčević Gladan et al., 2019). Overall, these observations suggest a more underlying and complex role of temperature in the occurrence of *O*. cf. *ovata* blooms, beyond a simple increasing facilitation with increasing temperature.

In a context of global warming, the investigation of the environmental niche of *O.* cf. *ovata* is key to help predicting bloom events and to plan efficient monitoring programs. A long-term monitoring dataset can provide a good comprehension of the potential link between environmental factors and *O*. cf. *ovata* bloom events. Such monitoring program was launched in Monaco (Ligurian Sea) in summer 2007, in order to assess the sanitary risk impact of *O*. cf. *ovata* on local recreational waters. This monitoring program is still ongoing and represents the world's largest time-series ever recorded for *O.* cf. *ovata* blooms. Data collected over the first two years of this monitoring program suggested a distinct pattern concerning the timing of the blooms and specific hydroclimatic conditions in that area (Cohu et al., 2011). Indeed, compared to 2008, 2007 was marked by a hot spring and a relatively cold summer and exhibited a strongly marked an earlier bloom episode

Here we conducted a multi-parametric approach to analyze the relationship between representative hydroclimatic parameters and *O.* cf. *ovata* bloom phenology in the NW

144 Mediterranean Sea, using a thirteen years monitoring dataset. Despite the large variability in
145 the phenological features of *O.* cf. *ovata* blooms, a specific link between SST and the bloom
146 phenology was found. We also explored the observations previously made by Cohu et al.
147 (2011) and describe its *in situ* thermal niche in NW Mediterranean Sea.

148

149 **2. Material and Methods**

150 2.1. Sampling site

151 Monaco is a sovereign city-state located on the French Riviera coast, in the NW
152 Mediterranean Sea. It is a highly touristic area whose population increases considerably
153 during the summer season. The Larvotto beach (43°44.71' N – 7°26.04' E) is a small
154 sheltered cove surrounded by residential buildings, shops and restaurants. The beach (Fig. 1)
155 is orientated South-East and artificial rocky dykes were built as a barrier to protect from
156 waves and swell. Such structures constitute ideal substrates for the development of ramified
157 structured macroalgae, especially Phaeophyceae and Florideophyceae, such as *Halopteris*
158 *scoparia* Sauvageau*, Dictyota* sp. Lamouroux and *Ellisolandia* sp. Hind & Saunders, which
159 host high densities of benthic microalgae including *O.* cf. *ovata.* Thus, neighbors and tourists
160 can be potentially exposed to the health risks associated to *O.* cf. *ovata* blooms. So far,
161 sporadic skin and mucosal irritations have been observed (Tichadou et al., 2010).

162

163 2.2. Sampling process and cell quantification

164 *O.* cf. *ovata* blooms occurring in the NW Mediterranean Sea are always observed in early
165 summer, when the SST increases and wind conditions are relatively calm. In order to quantify
166 the abundance of epiphytic *O.* cf. *ovata* cells, a monitoring program started in 2007 and was

then conducted every year, generally from mid-June until the end of August. The global estimation of the benthic cell stock in a given area is a complex task as the cell concentration may depend on the presence of certain types of macroalgae and may also vary according to small scale environmental changes. In order to give a reliable estimation of the cell abundance of this area, five different stations were sampled at each sampling date. The sampling campaign was carried out once a week during this period, between 9 am and 11 am, in five stations located on rocky substrate areas within the Larvotto Beach (see Fig. 1). The temporal evolution of the bloom was monitored through the estimation of both benthic cell stock and planktonic cell abundance quantification as described by Cohu et al. (2011). Samples of the most representative macroalgae (usually *Dictyota* sp., *Ellisolandia elongata* and/or *Halopteris scoparia*) were collected at 0.5-meter depth at each sampling station, by using 250 ml plastic flask filled up to the top with the surrounding water. Seawater above the sampled macroalgae, at 0.3-meter depth, was also collected for planktonic cell quantification. Plankton sampling was conducted before collecting the macroalgae in order to avoid releasing *Ostreopsis* benthic cells initially attached to the macroalgae which could overestimate *Ostreopsis* cells in the planktonic phase. All samples were then fixed with acidic Lugol (1% vol./vol.) and kept dark at 4°C. In the laboratory, macroalgae samples were vigorously shaken in the plastic flasks and the seawater was filtered through a 500 µm meshed filter to remove large macroalgal debris and isolate the epiphytic cells. Two additional rinsing of the macroalgae with 100 ml of 0.2 µm filtered seawater were conducted (with additional shaking and percolation steps) to detach as much microalgae cells as possible (Jauzein et al., 2018); all percolated water was merged and the total volume of seawater was noted. Macroalgae were then gently pressed to eliminate excess water and placed onto a tin foil for fresh weight measurement. Cell counts were performed on the percolated water of samples by using a light microscope (Zeiss, Oberkochen, Germany). A 1 ml Sedgwick Rafter counting chamber was used for the

epiphytic *Ostreopsis* cells and a 50 ml sedimentation column for the planktonic cells (Utermöhl, 1958). Benthic cell abundances were expressed as cells per gram of fresh weight of macroalgae (cell g^{-1} FW) and the plankton concentrations as cell l^{-1}.

2.3. Hydroclimatic parameters

During the sampling period, seawater temperature (± 0.1°C) was measured *in situ* at each station using a probe. The "Direction de l'Environnement" of Monaco provided hydroclimatic data from their meteorological program, including SST, salinity, pH, wind speed, wind direction and rainfall in Larvotto beach area. Wind speed and direction were used to represent South-North and West-East wind intensity vectors. In addition, long-term hydrological data including SST, nitrate and nitrite measurements from Point B in Villefranche-sur-Mer (43°41.10' N - 7°18.94' E) were collected by SOMLIT, a French national coastline monitoring network (http://somlit.fr). Located 12 km away from Monaco, Villefranche Bay can be considered as a reference area for the western part of the Ligurian Sea, including Monaco. These data were collected once a week in the bay, all year long, during the whole studied period.

2.4. Calculation and Statistics

Cell abundance for each sampling date was calculated as the mean cell abundance considering the five sampling stations. The difference in cell abundance between two sampling dates (i.e. net growth rate = μ) is the result of the combination of several parameters such as cell growth rate, cell dispersion, cell accumulation, predation and cell mortality rates. Net growth rates were calculated between each sampling week by using the following equation:

$$\mu = \frac{LnN2 - LnN1}{t2 - t1}$$

Where μ is the net growth rate (NGR, d^{-1}) between sampling day 1 and sampling day 2, N1 the mean cell abundance at sampling day 1 (cell g^{-1} FW), N2 the mean cell abundance at sampling day 2 (cell g^{-1} FW), t1 the date in days at the sampling date 1 and t2 the date in days at the sampling date 2. Note that this formula assumes an exponential growth (as defined in Wood et al., 2005) between the two sampling dates, although the detailed dynamics of the cell abundances is not possible to be tracked.

Data from year 2007 were not included in all the analyses as the monitoring started late in the year (early July) while the bloom was already declining. Starting date, maximum abundances and maximum growth rates could not be estimated for this year.

A mean weekly temperature profile was calculated over the thirteen-year monitoring period. Then, for each year, weekly SST anomalies were calculated as differences between temperature values and the mean weekly SST value. Finally, cumulative sums of SST anomalies were performed starting from the first week of each year.

Variations of net growth rate estimated during the phases of bloom development were analyzed as a function of SST using a non-parametric "loess" local polynomial regression model (Cleveland, 1979). The non-parametric Spearman correlation test was used to examine links between the abundance of benthic and planktonic *Ostreopsis* cells, as well as between SST and *O.* cf. *ovata* abundances (in the plankton and the benthos). A Wilcoxon signed-rank (non-parametric) test was applied on SST data collected both in Monaco and Villefranche Bay to ascertain the degree of similarity of the temperatures at both locations. A Principal Component Analysis (PCA) was used to explore the relationships between the different phenological features, namely, timing (starting date of the bloom), duration, intensity (characterized by the maximum cell abundances) and maximum growth rate of the bloom, and

environmental parameters (seawater temperature, salinity, winds, rainfall and nutrient concentrations). This PCA was performed using seasonal averages (mean of April, May and June) of environmental factors. These mean estimations were considered as representative of the hydroclimatic environment of the spring season, described as a crucial period before the bloom onset. The data set used for the PCA includes the years between 2008 and 2017 since rainfall, wind strength and nutrient concentrations data were not available for the last two years of monitoring. All statistical analyses were performed using R studio (R Core Team, 2019).

3. Results

3.1. Interannual variability

Blooms of *O.* cf. *ovata* occurred every year since 2007 at the same monitored site (Fig. 2). All data obtained over the last thirteen years of monitoring were pooled and the mean cell abundances were calculated over the five sampling stations. Results showed a positive correlation between *O.* cf. *ovata* benthic and planktonic abundances (Spearman test, N = 147, $r_s = 0.805$, p-value < 0.01) (Fig. 3). However, as explained earlier in the Introduction, *O.* cf. *ovata* is an epibenthic species, with the benthic fraction constituting the reservoir of the bloom. Therefore, the following analysis will focus exclusively on benthic abundances.

The highest abundance levels of *O.* cf. *ovata* blooms were constantly observed in summer (between June and August). Only two events within the thirteen-year time series showed two successive blooms in the same year: a first maximum peak of benthic cell abundance in summer followed by a second and smaller peak in late summer were observed in 2012 and 2013 (Fig. 2). Highly variable phenological features of the blooms were observed from one year to another (Fig. 2). Nevertheless, three main parameters enabled to distinguish

one bloom from another: the timing, the duration and the maximum cell abundance of blooms.

A concentration of 200,000 cells g^{-1} FW was estimated as the threshold above which the presence of *O.* cf. *ovata* was defined as a bloom. Indeed, this level refers to the lowest value of the overall maximum annual abundances measured during the thirteen blooms (212,300 cells g^{-1} FW measured in 2015). Since samples were collected only once a week, it was difficult to set the exact starting date of the bloom. The average starting day of a bloom was defined in the present study using the abundance threshold (200,000 cells g^{-1} FW) criterion and was defined on Julian day 191 (± 10.6). Delays occurred depending of the year, with blooms appearing as early as 15 days prior to this average starting day (Julian day 177, in 2015), while the latest bloom occurred 25 days later (Julian day 214, 2016).

The duration of the event was also variable over the years. When more than 200,000 cells g^{-1} FW were quantified during two consecutive sampling dates, the event was defined as a two-week bloom. When abundance values above this threshold were registered only once, then the event was defined as a one-week bloom. The blooms lasted in average 18.7 days (± 10.5), of which years 2011 and 2017 presented the longest blooming times (35 and 42 days respectively), and years 2007, 2009 and 2015 the shortest blooming times (7 days).

The highest annual maximum abundance values leveled to an average value of 570,878 (± 391,871) cells g^{-1} FW. However, the highest value ever recorded was 1,565,514 cells g^{-1} FW (174 % more than the average) in 2007 and the lowest value reached 212,300 cells g^{-1} FW (63 % less than the average) in 2013.

3.2. Relationship between environmental factors and interannual variability of *Ostreopsis* cf. *ovata* blooms

A multivariate analysis (PCA) was performed on data collected between April and June from the monitoring of environmental parameters, including physico-chemical measurements of water masses (SST, salinity, nutrients) as well as rainfall and wind intensity vectors (Table 1). The two first axis forming the first factorial space explained 70% of the total inertia of projected variables (Fig. 4), indicating a relatively good representation of the relationship between the different environmental parameters (Table 2). The most important variables for the construction of the first factorial axis of the PCA (46.2 % of the total inertia) were South-North winds (0.91), SST (-0.85) and West-East winds (0.74). The second axis was driven by nitrates (0.81), salinity (-0.63) and nitrites (0.56) and captured 23.5% of the variation. These results indicate that the first factorial axis of the PCA discriminates the years with bloom events according to the SST during the spring season. Indeed, years with high SST during spring seem to be related to low wind conditions. The second factorial axis highlights the nutrient loading of the area and discriminates years according to the nutrient availability during the spring seasons. Indeed, years which experience a high level of rainfall are related to high nitrate concentrations and low salinity values. Among the phenological features, the timing of the bloom event (bloom starting day) and the maximum annual growth rate are both correlated to the first axis of the PCA (0.71 and 0.39, respectively), while the intensity of the bloom (maximum cell concentration) is correlated to the second axis (0.41). No clear relation was found between environmental factors and the bloom duration.

Throughout the entire time series, the presence of *O.* cf. *ovata* benthic cells was observed when SST ranged between 18.2°C and 27.9°C, with an overall temperature average of 24.3 ± 1.8°C. When processing the entire dataset provided by the thirteen-year survey, blooming periods (i.e. when benthic cell abundance exceeded 200,000 cells g^{-1} FW) were identified when the mean SST reached 25.0 ± 1.5 °C. When focusing more specifically on each individual year, mean SST values measured during blooming periods ranged between

311 24.0 ± 1.5°C and 25.2 ± 1.7°C. At the very beginning of a bloom event, when cell densities
312 first exceeded the threshold of 200,000 cells g^{-1} FW, the average SST was estimated at 24.9
313 ±1.4°C.

314 Positive net growth rates (NGR) of *O.* cf. *ovata* were recorded when the SST varied
315 between 18.2°C and 27.9°C. A negative correlation was found between the temperature and
316 the NGR (Spearman, N = 133, r_s = -0.27, p-value < 0.01), but the relation was not linear and
317 highest positive NGRs were not associated to maximal temperature records (Fig. 5). Indeed,
318 the maximum NGR (0.53 d^{-1}) occurred at a temperature of 23.9°C. These variations are
319 confirmed by the local regression loess model, defining the optimal growth temperature at
320 23.5°C. In these terms, when considering each maximum NGR for each year, the window of
321 optimal growth temperature was estimated between 21.0°C and 24.7°C (Fig. 5).

322 No significant differences were found by comparing summer SST values measured in
323 Larvotto and in Villefranche Bay (Wilcoxon signed-rank test: N = 125, W = 3869, p-value =
324 0.645). Therefore, SST values recorded in Villefranche Bay were used as a proxy for
325 estimating the SST of Monaco area. In contrast to data collected in Monaco, SST
326 measurements in Villefranche Bay were collected weekly and throughout the year, which
327 enabled to describe the annual general hydroclimatic conditions of the area. Between 2007
328 and 2019, the annual mean SST was estimated at 18.8°C (± 4.3) and the respective mean
329 values of the lowest and the highest annual temperatures were estimated at 13.4°C (±0.4) and
330 26.3°C (±0.9), respectively. Annual SST anomalies were cumulated in order to compare the
331 heat accumulated in surface waters between each surveyed year (Fig. 6). Years with high
332 values of SST anomalies were considered as warmer, while years with low values of SST
333 anomalies were considered as cooler. Profiles of cumulated SST anomalies differed between
334 years but were also found to differ at a seasonal and monthly scale, thereby differentiating
335 years with a warmer spring season from years with a cooler spring. Amongst the previously

detailed phenological features of interest, strong positive correlations were found only between the bloom timing (starting of the event) and the cumulative sum of SST anomalies (Fig. 7A). This was observed for monthly averaged cumulative sum of SST anomalies over the months of April, May and June (prior to the bloom event) and during the whole spring season (April-May-June averaged values), but not before then (Fig. 7B). Thus, blooms of *O.* cf. *ovata* tend to start earlier in the season when SST anomalies are high. No other significant correlations were observed between SST anomalies and the duration of the bloom nor the maximum abundance of the bloom.

4. Discussion

Understanding the relationship between environmental parameters and the phenology of *O.* cf. *ovata* proliferations in the NW Mediterranean Sea can help predict either the timing, duration or intensity of blooms and hence support the management and mitigation of benthic HAB impacts. Such knowledge cannot be gained by observing one single bloom event (e.g. Vila et al., 2001; Battocchi et al., 2010; Totti et al., 2010; Accoroni et al., 2011; Illoul et al., 2012) but requires pluri-annual time series enabling to study the variability of occurring blooms along several years. Furthermore, long-term surveys as currently presented in this study enabled to characterize the *in situ* environmental niche of the target organism, *O.* cf. *ovata*, in the NW Mediterranean Sea. Such a set of data is of great interest for both modelers and managers, focusing on the prediction of HABs in the context of global change and warming of seawater surfaces.

In the present study, a multi-parametric approach and the analysis of environmental control parameters for algal growth were both assessed by using the benthic cell number data from *O.* cf. *ovata* abundance measurements. Indeed, as already reported by several studies conducted in NW Mediterranean regions (Mangialajo et al., 2008; Cohu et al., 2011; Jauzein et al., 2018), a strong correlation was found between concentrations of epiphytic and

planktonic cells of *O.* cf. *ovata*. *Ostreopsis* is recognized as a benthic organism adapted to the benthic life which is proven by its morphology and ecology (e.g., Hoppenrath et al., 2014). Due to the combination of possible internal biological rhythms and very local sea hydrodynamics, cells can detach from the benthos and circulate as pelagic cell, which explains the observed correlation between benthic and pelagic cell abundances. Epiphytic cells nevertheless represents the main stock, or reservoir, of the *O.* cf. *ovata* population able to sustain bloom events. In terms of toxic risks, both benthic and planktonic pools can be involved in direct contact skin irritations, but planktonic cells only would rather be the agents of intoxication events promoted by inhalation (Totti et al., 2010). In this case, *Ostreopsis*-produced toxic compounds would be spread by aerosolization and wind transport (Ciminiello et al., 2014).

Two main results emerge from the analysis of this long-term dataset and shall be discussed hereafter: (1) Spring SST were driving the timing of the bloom (starting date) and (2) the highest recorded temperatures were not correlated to the highest net growth rates of *O.* cf. *ovata*.

4.1. Interannual variations in bloom phenology

The monitoring of *O.* cf. *ovata* blooms which occurred in Monaco during thirteen successive summer seasons, revealed strong yearly variations in terms of phenological features. These variations, such as bloom timing, bloom length and bloom intensity, highlight the complexity behind the formation of *O.* cf. *ovata* blooms and the possible interactions between environmental parameters which are able to shape bloom events. The PCA analysis carried out on this data-set showed that the interannual variability in bloom timing and bloom maximum intensity could be explained by the combination of SSTs, nutrient loadings and wind regimes occurring in the spring season prior to the bloom initiation. Indeed, years which

386 experience high SSTs during the spring season are likely to see *O.* cf. *ovata* densities exceed
387 the 200,000 cells g^{-1} FW threshold early in the summer. High nutrient concentrations, prior
388 and during the bloom onset, is also likely to favor intense bloom episodes. Rainfall and
389 freshwater inflows obviously provided a high nutrient load and decreased water salinity, as
390 shown in the PCA. The combined action of SST and nutrient concentrations on *O.* cf. *ovata*
391 bloom phenology has also been investigated by Accoroni et al. (2015a) when studying a time-
392 series of *O.* cf. *ovata* blooms in the Northern Adriatic Sea. These authors suggested that the
393 bloom onset could be triggered when the SST reached a certain threshold and simultaneously
394 coinciding with an inflow of P-riche waters which occurred after a period of relatively high
395 N:P ratio. Similar interconnections were observed by Bucci et al. (2020) regarding the
396 phenology of *Alexandrium catenella* blooms which occurred in the Bay of Fundy (Gulf of
397 Maine, NW Atlantic). The study showed that the bloom timing and the date exhibiting the
398 maximum cell density (bloom intensity) varied between the years and suggested that both
399 parameters could be linked to a high input of freshwater during the spring and that warmer
400 years were likely to earlier initiate the timing of blooms. In our study, spring season
401 hydrodynamics induced by the strength and the direction of winds did not significantly impact
402 the variability of *O.* cf. *ovata* phenological features. This latter observation was described at
403 least at the interannual scale, although it may play a more important role in the bloom
404 development at the seasonal scale. However, these environmental parameters were shown to
405 be related to high SSTs. Indeed, in the NW Mediterranean seas, wind regimes coming from
406 the South are generally warm and thereby increase the water temperature. Our analysis also
407 highlights the importance of the spring season regarding the phenology of recurrent summer
408 bloom events. Even though environmental factors strongly impact the phenology of the bloom
409 when it is occurring, less is known about how hydroclimatic parameters are affecting the
410 bloom phenology prior to its development.

411 Further investigations of factors initiating the bloom revealed a strong positive
412 correlation between cumulated SST anomalies and the starting day of the bloom. This relation
413 confirms that *O.* cf. *ovata* blooms are likely to occur earlier in the year, when spring SST are
414 warmer than usual. This correlation is even stronger and more significant when approaching
415 the summer season. Indeed, from April onwards, temperature anomalies can be cumulated to
416 predict the most favorable period for epiphytic *O.* cf. *ovata* abundances to reach the 200,000
417 cells g^{-1} FW threshold. However, variations in SST during the months of May and June have a
418 strong impact on the bloom timing and may reject the prediction from April. It hence appears
419 that the accuracy for predicting the bloom with SST parameter gets stronger when
420 approaching the bloom event.

421 The occurrence of an early bloom can be explained by an early germination of resting
422 *O.* cf. *ovata* cysts and/or by a higher division rate favored by optimal environmental
423 conditions for algal growth. For instance, Lau et al. (2017) showed that an intense bloom of
424 *Alexandrium minutum,* which occurred in the northeast of the Peninsular Malaysian waters,
425 was presumably initiated by an active excystment process. Indeed, several environmental
426 parameters have already shown to trigger dinoflagellate cyst germination such as light
427 exposure (Anderson et al., 1987; Moore et al., 2015), nutrient availability (Bravo and
428 Anderson, 1994; Binder and Anderson, 2004) and a mandatory exposed period to dark-cold
429 conditions (Montresor and Lewis, 2006). Temperature also appears to be one of the main
430 factors controlling excystment of resting dinoflagellate cells (Anderson, 1980; Bravo and
431 Anderson, 1994; Ní Rathaille and Raine, 2011; Moore et al., 2015) as dinoflagellate cysts
432 require a certain SST threshold in order to induce excystment. For *O.* cf. *ovata* blooms in the
433 Mediterranean Sea, no relationship between the bloom starting date and neither SST nor
434 nutrient concentrations was found. Instead, only cumulated temperature anomalies
435 (illustrations of heat accumulation in surface waters) showed effects on the bloom timing.

436 Accoroni et al. (2014) indicated that cysts of *O.* cf. *ovata,* sampled from the N Adriatic Sea,
437 needed a temperature of 25°C to germinate, which could explain why blooms occurring in
438 this area are observed from late summer to beginning of fall, after recording the highest
439 temperatures. Another study conducted by Accoroni et al. (2015a) suggested that the
440 combination of optimal temperature and Nitrate/Phosphate ratio could favor both the initiation
441 of cell excystment and cell proliferation, therefore triggering the bloom onset. In this study
442 monitoring *O.* cf. *ovata* blooms in the Conero Riviera (N Adriatic Sea) between 2007 and
443 2012, cells were never observed below 25°C prior to the bloom onset. Conversely, in
444 Monaco, cells of *O.* cf. *ovata* have been observed at temperatures as low as 18.2°C, and
445 blooms usually start before the maximum SSTs are reached. These variable results seem to
446 indicate that depending on the geographical location, different SST thresholds might be
447 necessary for triggering the cyst germination process which leads to an *O.* cf. *ovata* bloom.

448 *O.* cf. *ovata* bloom events also varied in duration and in intensity across the years.
449 During the bloom events, the highest measured abundance of epiphytic cells reached more
450 than 1,500,000 cells g^{-1} FW (in 2007) while the lowest maximum abundance barely exceeded
451 200,000 cells g^{-1} FW (in 2013). The blooms lasted from less than one week (only one
452 sampling day, in 2009 and 2015) up to 4 weeks (5 consecutive sampling days, in 2011).
453 Length and intensity of blooms are the results of a balance between production of biomass
454 (gross growth rate) *versus* induction of cell quiescence (encystment) and cell loss. Diverse
455 factors can induce a limitation of microalgal growth or activation of encystment or lysis.
456 These factors can either be abiotic, such as strong hydrodynamics, nutrient depletion or
457 extreme temperatures, or biotic (e.g., grazing, parasitic interactions). Therefore, long lasting
458 and intense bloom episodes could be the result of persisting optimal hydroclimatic conditions
459 over a long enough period which enhances the production of biomass, and this combined to
460 low biotic (grazers, parasites) and abiotic (hydrodynamics) pressures which are responsible

461 for cell loss. Temporary cyst formation could be a strategy leading to maintain blooms
462 throughout time. Indeed, *O.* cf. *ovata* can form temporary cysts from vegetative cells
463 (Accoroni et al., 2014) when biotic or abiotic pressures emerge in order to overcome short
464 periods of stress. This mechanism has already been shown to help maintain blooms of other
465 harmful dinoflagellate such as *Alexandrium taylori* (Garcés, 2002). Another strategy would be
466 the fueling of the bloom by resting cysts throughout the bloom event, as observed in
467 *Alexandrium* species (Anglès et al., 2012; Lau et al., 2017). By undergoing a slow and wide
468 excystment process, the resting cyst stock would hence continuously provide new vegetative
469 cells to the blooming population, and *in fine* enable a longer bloom episode.

470 In addition to the numerous environmental factors responsible for *O.* cf. *ovata* bloom
471 phenology, part of the variability observed in bloom dynamics over the years may be the
472 result of the strong small-scale repartition of cells on the benthos. Variations observed in the
473 *O.* cf. *ovata* bloom phenology could be related to a high variability of cell abundances
474 measured over small spatial scales. Indeed, the patchy distribution of epiphytic *O.* cf. *ovata*
475 cells, directly linked to the distribution of their biotic substrate, makes the accurate estimation
476 of the benthic cell stock of a given area challenging. This has already been observed by Cohu
477 et al. (2011), who carried out the first two years of this present monitoring program, and
478 suggested that bloom phenology could be related to the spatial and temporal evolution of the
479 diversity of biotic substrates (Totti et al., 2010), as well as local hydrodynamic conditions. A
480 similar monitoring study was conducted in the Gulf of Naples, in the Tyrrhenian Sea
481 (Mediterranean Sea), aimed to assess the temporal variability of *O.* cf. *ovata* (Di Ciocco,
482 2015). Strong variations in abundances were observed throughout their seasonal monitoring
483 but no clear effect of environmental factors, including sea temperature, on the phenology of
484 *O.* cf. *ovata* was found.

485 Finally, although SST is recognized as a determinant factor for the development of
486 benthic dinoflagellate cells (Pistocchi et al., 2011; Parsons et al., 2012), *O.* cf. *ovata*
487 abundances and growth rates measured during the bloom events are also under the control of
488 other environmental parameters (Carnicer et al., 2015; Accoroni and Totti, 2016). It is
489 generally agreed that *O.* cf. *ovata* blooms are favored by low hydrodynamic conditions, since
490 the highest abundance levels are rather recorded in sheltered areas, even though blooms have
491 also been observed in exposed sites (Barone, 2007; Totti et al., 2010; Accoroni and Totti,
492 2016). By comparing bloom events throughout the years, the PCA analysis in this present
493 study showed no straight forward relation between environmental parameters and maximum
494 annual growth rates of *O.* cf. *ovata*.
495

496 4.2. Net growth rate

497 Throughout the recurrent *O.* cf. *ovata* summer bloom episodes, the highest positive net
498 growth rates did not coincide with the highest recorded SST. This indicates that relatively
499 high temperatures are not necessarily optimal for the growth of *Ostreopsis*, at least in the
500 Monaco area. Instead, the loess regression model indicated that a moderate temperature
501 (23.5°C) was most suitable for *O.* cf. *ovata* growth. Numerous *in situ* studies have already
502 tried to understand the relation between SST and bloom development, often resulting in
503 different conclusions which seem to depend on the actual studied location (Accoroni and
504 Totti, 2016). For instance, in the NW Mediterranean Sea, the highest abundances of *O.* cf.
505 *ovata* were recorded when temperatures were either higher than 26°C (e.g., in the Ligurian
506 Sea (Mangialajo et al., 2008) and in Greece (Aligizaki and Nikolaidis, 2006)) or below 23°C
507 (e.g., in the Northern Adriatic Sea (Totti et al., 2010; Accoroni et al., 2011)). In most of these
508 studies, the monitored data were reported as cell abundances and did not show any direct
509 correlation between SST and cell concentration (Vila et al., 2001; Totti et al., 2010; Cohu et

al., 2011). On the other hand, by estimating the maximum growth rate of *O.* cf. *ovata* over successive bloom events in this present study focusing on the NW Mediterranean Sea, a narrower range of optimal growth temperatures was defined between 21.0°C and 24.7°C. This temperature range is in agreement with results obtained from laboratory scale studies, which reported that optimal growth temperatures could be strain specific and part of such a strain specificity referring to a thermal niche could depend on the studied area. For instance, Pezzolesi et al. (2012) showed that strains collected in the Tyrrhenian Sea showed maximum growth rates at 20°C whereas highest growth rates were observed at 24°C and 30°C when studying strains isolated from the Catalan coast (Spain, Carnicer et al., 2016) and the Adriatic Sea (Granéli et al., 2011), respectively. However, even within the same region of the Mediterranean Sea, temperature niches enabling optimal growth seem to vary depending on the strain. Indeed, a laboratory study carried out by Scalco et al., (2012) on strains collected in the Tyrrhenian and Adriatic seas showed that the optimal temperature for algal growth was strain-specific, varying between 22°C and 26°C depending on the clone. Since *O.* cf. *ovata* niche temperatures are strongly variable depending on the location but also depending on the strains across Mediterranean Sea, the impact of temperature on the development of blooms are likely to vary depending on local environmental parameters and clonal diversity. In addition, the highest growth rates of *O.* cf. *ovata* do not coincide with the highest observed SSTs, as also reported in most of the *in situ* and laboratory studies conducted in the Mediterranean Sea. This suggests a more complex role of temperature conditions on the phenology of the blooms than a simple increasing bloom facilitation due to increasing temperature. Exceeding too high SST values might even limit the development of the bloom. In the context of ocean warming, this has to be taken into account in the view of implementing long-term previsions of *O.* cf. *ovata* bloom events in the future.

4.3.Spring SST anomalies and *in situ* thermal niche: a tool for modelers and managers

Relationships between the phenology of *O.* cf. *ovata* blooms and environmental parameters described in this present study are of great interest for predicting and managing HABs. Indeed, the correlation between spring SST anomalies and bloom timing represents a useful tool for predicting future *O.* cf. *ovata* HABs in the Monaco area. Using SST data recorded during the beginning of the year enabled to predict a temporal window for the beginning of a bloom event which can be useful to guide the monitoring effort (Fig. 7A). The *in situ* thermal niche, determined by the relationship between SST and net growth rates during bloom episodes, could also be used by modelers to forecast the future evolution of both the bloom phenology and distribution which can be notably impactful when facing increasing sea temperatures.

Modeling the dynamics of coastal HABs is crucial, especially in a context of climate change where the occurrence of HABs seems to be increasing in numbers and expanding in space. Many authors are trying to understand and to predict blooms of toxic dinoflagellates (Maguire et al., 2016; Moita et al., 2016; Ruiz-Villarreal et al., 2016) and toxic cyanobacteria (Hamilton et al., 2009; Rigosi et al., 2015) by using models based on ecological observations. Until now, the accuracy in modelling and predicting such complex phenological events seems to be limited by the lack of available data describing both the species itself and the environmental parameters, but also by the numerous pending questions regarding the ecology of *O.* cf. *ovata* (Asnaghi et al., 2012). Although our study provides data on the actual temperature niche of *O.* cf. *ovata* in the NW Mediterranean Sea and the relations between the bloom phenology and spring SST temperatures, more models describing *O.* cf. *ovata* blooms still need to be designed, improved and adapted to local environmental variables in order to minimize the risks to be exposed to such events. The determination of the thermal niche of *O.* cf. *ovata* in the NW Mediterranean Sea could help forecasting potential long-term variations in the phenology of the blooms but also a possible evolution of the distribution of blooms. On

the other hand, the short-term prediction of bloom timing could provide a substantial support to local sanitary authorities in charge of toxic outbreaks, as this could be used to estimate potential risks of exposure weeks before the beginning of the bloom and hence to gain precious time for deploying management strategies.

Regarding the impact of climate change, many studies consider global warming as a potential enhancement factor for benthic HABs species to expand their geographical areas, increase the seasonal occurrences and bloom windows (Wells et al., 2015; Gobler et al., 2017; Nakada et al., 2018; Gobler, 2020; Tester et al., 2020). In the Mediterranean Sea, climate projections foresee an increase in SSTs, with an average of 0.45°C per decade by 2050 (Alexander et al., 2018). Geographical expansion towards higher latitudes in the Mediterranean Sea is not possible, since *O.* cf. *ovata* is already found in the northern parts of the NW Mediterranean Sea. Moreover, an increase in SST temperature may not necessarily result in more intense blooms since this present study has shown that the highest SSTs do not coincide with the highest growth rates. Therefore, the assumption that ocean warming shall favor the development and the expansion of *O.* cf. *ovata* species and blooms in the future seems more complex than previously thought. On the other hand, global warming could favor an earlier bloom, as optimal temperature conditions would be reached earlier in the season. Global warming is not the only consequence of climate change and more specific studies between *O.* cf. *ovata* and future ecological conditions in the Mediterranean Sea are needed.

5. Conclusion

The phenology of *O.* cf. *ovata* blooms is governed by a complex assemblage of environmental factors and is still lacking specific knowledge able to describe how these environmental parameters interact and affect the progress of toxic blooms. The present study is based on a

584 13-year time-series of *O.* cf. *ovata* blooms in Monaco and reveals that part of the interannual
585 variability of bloom phenological features, such as the bloom timing and the maximum
586 intensity of the bloom, could be explained by a combination of environmental parameters,
587 including SST and nutrient concentrations, especially during the spring season. The optimal
588 growth temperature which favors the *O.* cf. *ovata* blooms in NW Mediterranean waters has
589 been estimated between 21°C and 25°C. In addition, this study revealed a clear relation
590 between spring SSTs and the timing of the bloom of *O.* cf. *ovata* occurring in the NW
591 Mediterranean region. By processing data from this longest time series dedicated to *O.* cf.
592 *ovata* blooms, results suggest that the accumulation of positive SST anomalies induces an
593 early start of the bloom. Considering the increasing trend of SST observed worldwide, due to
594 global climatic changes, such results could be of a great interest for the prediction and
595 management of *O.* cf. *ovata* blooms in recreational waters. Further data collection in the scope
596 of this time series is needed to improve the present knowledge and to deepen investigations
597 regarding the effect of combined environmental parameters on *O.* cf. *ovata* bloom phenology.

598 **Authors' contribution**

599 K.D., A-S.P., S.M. V.D-S. and R.L. designed and contributed to the conduction of the
600 monitoring campaign. K.D., A-S.P. and S.M. analyzed the samples. K.D. and S.G. designed
601 and performed the modelling and statistical analyses. K.D., S.G., E.B., C.J., R.S. and R.L.
602 analyzed the results and prepared the figures. K.D. and R.L. wrote the first version of the
603 manuscript. All authors reviewed and accepted the final version of the manuscript.

604 **Acknowledgement**

605 This work was carried out in the frame the PhD thesis of K.D., supported by the project
606 CoCliME which is part of ERA4CS, an ERA-NET initiated by JPI Climate, and funded by
607 EPA (IE), ANR (FR), BMBF (DE), UEFISCDI (RO), RCN (NO) and FORMAS (SE), with

608 co-funding by the European Union (Grant 690462). The monitoring program in the Larvotto
609 Beach was funded by the "Direction de l'Environnement" of Monaco. We are deeply grateful
610 to all people involved in sample collection and analysis over the monitoring period for their
611 precious help without whom this long-term study could not have been conducted. We are also
612 grateful to the "Direction de l'Environnement" of Monaco and to SOMLIT (French National
613 Service of Coastal Long-Term Marine Observation, https://www.somlit.fr/) for providing us
614 hydroclimatic data. French authors are part of GDR PHYCOTOX, a CNRS/IFREMER
615 network on HAB.

616

617

618

619

620

621 **References**

622 Abdennadher, M., Zouari, A.B., Sahnoun, W.F., Alverca, E., Penna, A., Hamza, A., 2017.
623 *Ostreopsis* cf. *ovata* in the Gulf of Gabès (south-eastern Mediterranean Sea):
624 morphological, molecular and ecological characterization. Harmful Algae 63, 56–67.
625 https://doi.org/10.1016/j.hal.2017.01.009
626 Accoroni, S., Colombo, F., Pichierri, S., Romagnoli, T., Marini, M., Battocchi, C., Penna, A.,
627 Totti, C., 2012. Ecology of *Ostreopsis* cf. *ovata* Blooms in the Northwestern Adriatic
628 Sea. Cryptogam. Algol. 33, 191–198. https://doi.org/10.7872/crya.v33.iss2.2011.191
629 Accoroni, S., Glibert, P.M., Pichierri, S., Romagnoli, T., Marini, M., Totti, C., 2015a. A
630 conceptual model of annual *Ostreopsis* cf. *ovata* blooms in the northern Adriatic Sea
631 based on the synergic effects of hydrodynamics, temperature, and the N:P ratio of
632 water column nutrients. Harmful Algae 45, 14–25.
633 https://doi.org/10.1016/j.hal.2015.04.002
634 Accoroni, S., Percopo, I., Cerino, F., Romagnoli, T., Pichierri, S., Perrone, C., Totti, C.,
635 2015b. Allelopathic interactions between the HAB dinoflagellate *Ostreopsis* cf. *ovata*
636 and macroalgae. Harmful Algae 49, 147–155.
637 https://doi.org/10.1016/j.hal.2015.08.007

638 Accoroni, S., Romagnoli, T., Colombo, F., Pennesi, C., Di Camillo, C.G., Marini, M.,
639 Battocchi, C., Ciminiello, P., Dell'Aversano, C., Dello Iacovo, E., Fattorusso, E.,
640 Tartaglione, L., Penna, A., Totti, C., 2011. *Ostreopsis* cf. *ovata* bloom in the northern
641 Adriatic Sea during summer 2009: Ecology, molecular characterization and toxin
642 profile. Mar. Pollut. Bull. 62, 2512–2519.
643 https://doi.org/10.1016/j.marpolbul.2011.08.003
644 Accoroni, S., Romagnoli, T., Pichierri, S., Totti, C., 2014. New insights on the life cycle
645 stages of the toxic benthic dinoflagellate *Ostreopsis* cf. *ovata*. Harmful Algae 34, 7–
646 16. https://doi.org/10.1016/j.hal.2014.02.003
647 Accoroni, S., Totti, C., 2016. The toxic benthic dinoflagellates of the genus *Ostreopsis* in
648 temperate areas: a review. Adv. Oceanogr. Limnol. 7, 1–15.
649 https://doi.org/10.4081/aiol.2016.5591
650 Accoroni, S., Totti, C., Razza, E., Congestri, R., Campanelli, A., Marini, M., Ellwood,
651 N.T.W., 2017. Phosphatase activities of a microepiphytic community during a bloom
652 of *Ostreopsis* cf. *ovata* in the northern Adriatic Sea. Water Res. 120, 272–279.
653 https://doi.org/10.1016/j.watres.2017.05.004
654 Alexander, M.A., Scott, J.D., Friedland, K.D., Mills, K.E., Nye, J.A., Pershing, A.J., Thomas,
655 A.C., 2018. Projected sea surface temperatures over the 21stcentury: Changes in the
656 mean, variability and extremes for large marineecosystem regions of Northern Oceans.
657 Elem Sci Anth 6, 9. https://doi.org/10.1525/elementa.191
658 Aligizaki, K., Katikou, P., Nikolaidis, G., Panou, A., 2008. First episode of shellfish
659 contamination by palytoxin-like compounds from *Ostreopsis* species (Aegean Sea,
660 Greece). Toxicon 51, 418–427. https://doi.org/10.1016/j.toxicon.2007.10.016
661 Aligizaki, K., Nikolaidis, G., 2006. The presence of the potentially toxic genera *Ostreopsis*
662 and *Coolia* (Dinophyceae) in the North Aegean Sea, Greece. Harmful Algae 5, 717–
663 730. https://doi.org/10.1016/j.hal.2006.02.005
664 Anderson, D.M., 1980. Effects of temperature conditioning on development and germination
665 of *Gonyaulax tamarensis* (dinophyceae) hypnozygotes. J. Phycol. 16, 166–172.
666 https://doi.org/10.1111/j.1529-8817.1980.tb03013.x
667 Anderson, D.M., Cembella, A.D., Hallegraeff, G.M., 2012. Progress in Understanding
668 Harmful Algal Blooms: Paradigm Shifts and New Technologies for Research,
669 Monitoring, and Management. Annu. Rev. Mar. Sci. 4, 143–176.
670 https://doi.org/10.1146/annurev-marine-120308-081121
671 Anderson, D.M., Glibert, P.M., Burkholder, J.M., 2002. Harmful algal blooms and
672 eutrophication: Nutrient sources, composition, and consequences. Estuaries 25, 704–
673 726. https://doi.org/10.1007/BF02804901
674 Anderson, D.M., Taylor, C.D., Armbrust, E.V., 1987. The effects of darkness and
675 anaerobiosis on dinoflagellate cyst germination: Dinoflagellate cyst germination.
676 Limnol. Oceanogr. 32, 340–351. https://doi.org/10.4319/lo.1987.32.2.0340
677 Anglès, S., Garcés, E., Reñé, A., Sampedro, N., 2012. Life-cycle alternations in *Alexandrium*
678 *minutum* natural populations from the NW Mediterranean Sea. Harmful Algae 16, 1–
679 11. https://doi.org/10.1016/j.hal.2011.12.006
680 Asnaghi, V., Bertolotto, R., Giussani, V., Mangialajo, L., Hewitt, J., Thrush, S., Moretto, P.,
681 Castellano, M., Rossi, A., Povero, P., Cattaneo-Vietti, R., Chiantore, M., 2012.
682 Interannual Variability in *Ostreopsis ovata* Bloom Dynamic along Genoa Coast
683 (North-Western Mediterranean): A Preliminary Modeling Approach. Cryptogam.
684 Algol. 33, 181–189. https://doi.org/10.7872/crya.v33.iss2.2011.181
685 Barone, R., 2007. Behavioural trait of *Ostreopsis ovata* (Dinophyceae) in Mediterranean rock
686 pools: the spider's strategy. Harmful Algae News 33, 1–3.

687 Barroso García, P., Rueda de la Puerta, P., Parrón Carreño, T., Marín Martínez, P., Guillén
688 Enríquez, J., 2008. An epidemic outbreak with respiratory symptoms in the province
689 of Almeria (Spain) due to toxic microalgae exposure. Gac. Sanit. 22, 578–584.
690 Battocchi, C., Totti, C., Vila, M., Masó, M., Capellacci, S., Accoroni, S., Reñé, A., Scardi,
691 M., Penna, A., 2010. Monitoring toxic microalgae *Ostreopsis* (dinoflagellate) species
692 in coastal waters of the Mediterranean Sea using molecular PCR-based assay
693 combined with light microscopy. Mar. Pollut. Bull. 60, 1074–1084.
694 https://doi.org/10.1016/j.marpolbul.2010.01.017
695 Binder, B.J., Anderson, D.M., 2004. Physiological and environmental control of germination
696 in *Scrippsiella trochoidea* (dinophyceae) resting cysts1. J. Phycol. 23, 99–107.
697 https://doi.org/10.1111/j.0022-3646.1987.00099.x
698 Biré, R., Trotereau, S., Lemée, R., Delpont, C., Chabot, B., Aumond, Y., Krys, S., 2013.
699 Occurrence of palytoxins in marine organisms from different trophic levels of the
700 French Mediterranean coast harvested in 2009. Harmful Algae 28, 10–22.
701 https://doi.org/10.1016/j.hal.2013.04.007
702 Biré, R., Trotereau, S., Lemée, R., Oregioni, D., Delpont, C., Krys, S., Guérin, T., 2015. Hunt
703 for Palytoxins in a Wide Variety of Marine Organisms Harvested in 2010 on the
704 French Mediterranean Coast. Mar. Drugs 13, 5425–5446.
705 https://doi.org/10.3390/md13085425
706 Blanfuné, A., Boudouresque, C.F., Grossel, H., Thibaut, T., 2015. Distribution and abundance
707 of *Ostreopsis* spp. and associated species (Dinophyceae) in the northwestern
708 Mediterranean: the region and the macroalgal substrate matter. Environ. Sci. Pollut.
709 Res. 22, 12332–12346. https://doi.org/10.1007/s11356-015-4525-4
710 Bravo, I., Anderson, D.M., 1994. The effects of temperature, growth medium and darkness on
711 excystment and growth of the toxic dinoflagellate *Gymnodinium catenatum* from
712 northwest Spain. J. Plankton Res. 16, 513–525.
713 https://doi.org/10.1093/plankt/16.5.513
714 Brescianini, C., Grillo, C., Melchiorre, N., Bertolotto, R., Ferrari, A., Vivaldi, B., Icardi, G.,
715 Gramaccioni, L., Funari, E., Scardala, S., 2006. *Ostreopsis ovata* algal blooms
716 affecting human health in Genova, Italy, 2005 and 2006. Euro Surveill. Bull. Eur. Sur
717 Mal. Transm. Eur. Commun. Dis. Bull. 11, E060907.3.
718 Brissard, C., Herrenknecht, C., Séchet, V., Hervé, F., Pisapia, F., Harcouet, J., Lémée, R.,
719 Chomérat, N., Hess, P., Amzil, Z., 2014. Complex Toxin Profile of French
720 Mediterranean *Ostreopsis* cf. *ovata* Strains, Seafood Accumulation and Ovatoxins
721 Prepurification. Mar. Drugs 12, 2851–2876. https://doi.org/10.3390/md12052851
722 Bucci, A.F., Thomas, A.C., Cetinić, I., 2020. Interannual Variability in the Thermal Habitat of
723 *Alexandrium* catenella in the Bay of Fundy and the Implications of Climate Change.
724 Front. Mar. Sci. 7, 587990. https://doi.org/10.3389/fmars.2020.587990
725 Carnicer, O., García-Altares, M., Andree, K.B., Tartaglione, L., Dell'Aversano, C.,
726 Ciminiello, P., de la Iglesia, P., Diogène, J., Fernández-Tejedor, M., 2016. *Ostreopsis*
727 cf. *ovata* from western Mediterranean Sea: Physiological responses under different
728 temperature and salinity conditions. Harmful Algae 57, 98–108.
729 https://doi.org/10.1016/j.hal.2016.06.002
730 Carnicer, O., Guallar, C., Andree, K.B., Diogène, J., Fernández-Tejedor, M., 2015. *Ostreopsis*
731 cf. *ovata* dynamics in the NW Mediterranean Sea in relation to biotic and abiotic
732 factors. Environ. Res. 143, 89–99. https://doi.org/10.1016/j.envres.2015.08.023
733 Ciminiello, P., Dell'Aversano, C., Dello Iacovo, E., Fattorusso, E., Forino, M., Grauso, L.,
734 Tartaglione, L., Guerrini, F., Pezzolesi, L., Pistocchi, R., Vanucci, S., 2012. Isolation
735 and Structure Elucidation of Ovatoxin-a, the Major Toxin Produced by *Ostreopsis*
736 *ovata*. J. Am. Chem. Soc. 134, 1869–1875. https://doi.org/10.1021/ja210784u

737 Ciminiello, P., Dell'Aversano, C., Fattorusso, E., Forino, M., Magno, G.S., Tartaglione, L.,
738 Grillo, C., Melchiorre, N., 2006. The Genoa 2005 Outbreak. Determination of Putative
739 Palytoxin in Mediterranean *Ostreopsis ovata* by a New Liquid Chromatography
740 Tandem Mass Spectrometry Method. Anal. Chem. 78, 6153–6159.
741 https://doi.org/10.1021/ac060250j
742 Ciminiello, P., Dell'Aversano, C., Iacovo, E.D., Fattorusso, E., Forino, M., Tartaglione, L.,
743 Benedettini, G., Onorari, M., Serena, F., Battocchi, C., Casabianca, S., Penna, A.,
744 2014. First Finding of *Ostreopsis* cf. *ovata* Toxins in Marine Aerosols. Environ. Sci.
745 Technol. 48, 3532–3540. https://doi.org/10.1021/es405617d
746 Cleveland, W.S., 1979. Robust Locally Weighted Regression and Smoothing Scatterplots. J.
747 Am. Stat. Assoc. 74, 829–836. https://doi.org/10.1080/01621459.1979.10481038
748 Cohu, S., Lemée, R., 2012. Vertical distribution of the toxic epibenthic dinoflagellates
749 *Ostreopsis* cf. *ovata*, *Prorocentrum lima* and *Coolia monotis* in the NW Mediterranean
750 Sea. Cah. Biol. Mar. 55, 373–380.
751 Cohu, S., Mangialajo, L., Thibaut, T., Blanfuné, A., Marro, S., Lemée, R., 2013. Proliferation
752 of the toxic dinoflagellate *Ostreopsis* cf. *ovata* in relation to depth, biotic substrate and
753 environmental factors in the North West Mediterranean Sea. Harmful Algae 24, 32–
754 44. https://doi.org/10.1016/j.hal.2013.01.002
755 Cohu, S., Thibaut, T., Mangialajo, L., Labat, J.-P., Passafiume, O., Blanfuné, A., Simon, N.,
756 Cottalorda, J.-M., Lemée, R., 2011. Occurrence of the toxic dinoflagellate *Ostreopsis*
757 cf. *ovata* in relation with environmental factors in Monaco (NW Mediterranean). Mar.
758 Pollut. Bull. 62, 2681–2691. https://doi.org/10.1016/j.marpolbul.2011.09.022
759 David, H., Ganzedo, U., Laza-Martínez, A., Orive, E., 2012. Relationships between the
760 Presence of *Ostreopsis* (Dinophyceae) in the Atlantic Coast of the Iberian Peninsula
761 and Sea-Surface Temperature. Cryptogam. Algol. 33, 199–207.
762 https://doi.org/10.7872/crya.v33.iss2.2011.199
763 Davidson, K., Gowen, R.J., Harrison, P.J., Fleming, L.E., Hoagland, P., Moschonas, G., 2014.
764 Anthropogenic nutrients and harmful algae in coastal waters. J. Environ. Manage. 146,
765 206–216. https://doi.org/10.1016/j.jenvman.2014.07.002
766 Di Cioccio, D., 2015. Ecology of the toxic dinoflagellate *Ostreopsis* cf. *ovata* along the coasts
767 of the Campania region (Tyrrhenian Sea, Mediterranean Sea).
768 https://doi.org/10.6092/UNINA/FEDOA/10371
769 Durando, P., Ansaldi, F., Oreste, P., Moscatelli, P., Marensi, L., Grillo, C., Gasparini, R.,
770 Icardi, G., Collaborative Group for the Ligurian Syndromic Algal Surveillance, 2007.
771 *Ostreopsis ovata* and human health: epidemiological and clinical features of
772 respiratory syndrome outbreaks from a two-year syndromic surveillance, 2005-06, in
773 north-west Italy. Euro Surveill. Bull. Eur. Sur Mal. Transm. Eur. Commun. Dis. Bull.
774 12, E070607.1.
775 Faust, M.A., Morton, S.L., Quod, J.P., 1996. Further sem study of marine dinoflagellates: the
776 genus *Ostreopsis* (dinophyceae)1. J. Phycol. 32, 1053–1065.
777 https://doi.org/10.1111/j.0022-3646.1996.01053.x
778 Fu, F., Tatters, A., Hutchins, D., 2012. Global change and the future of harmful algal blooms
779 in the ocean. Mar. Ecol. Prog. Ser. 470, 207–233. https://doi.org/10.3354/meps10047
780 Garces, E., 2002. Role of temporary cysts in the population dynamics of *Alexandrium* taylori
781 (Dinophyceae). J. Plankton Res. 24, 681–686. https://doi.org/10.1093/plankt/24.7.681
782 Giussani, V., Asnaghi, V., Pedroncini, A., Chiantore, M., 2017. Management of harmful
783 benthic dinoflagellates requires targeted sampling methods and alarm thresholds.
784 Harmful Algae 68, 97–104. https://doi.org/10.1016/j.hal.2017.07.010

785 Glibert, P., Seitzinger, S., Heil, C., Burkholder, J., Parrow, M., Codispoti, L., Kelly, V., 2005.
786 The Role of Eutrophication in the Global Proliferation of Harmful Algal Blooms.
787 Oceanography 18, 198–209. https://doi.org/10.5670/oceanog.2005.54
788 Glibert, P.M., Icarus Allen, J., Artioli, Y., Beusen, A., Bouwman, L., Harle, J., Holmes, R.,
789 Holt, J., 2014. Vulnerability of coastal ecosystems to changes in harmful algal bloom
790 distribution in response to climate change: projections based on model analysis. Glob.
791 Change Biol. 20, 3845–3858. https://doi.org/10.1111/gcb.12662
792 Gobler, C.J., 2020. Climate Change and Harmful Algal Blooms: Insights and perspective.
793 Harmful Algae 91, 101731. https://doi.org/10.1016/j.hal.2019.101731
794 Gobler, C.J., Doherty, O.M., Hattenrath-Lehmann, T.K., Griffith, A.W., Kang, Y., Litaker,
795 R.W., 2017. Ocean warming since 1982 has expanded the niche of toxic algal blooms
796 in the North Atlantic and North Pacific oceans. Proc. Natl. Acad. Sci. 114, 4975–4980.
797 https://doi.org/10.1073/pnas.1619575114
798 Granéli, E., Vidyarathna, N.K., Funari, E., Cumaranatunga, P.R.T., Scenati, R., 2011. Can
799 increases in temperature stimulate blooms of the toxic benthic dinoflagellate
800 *Ostreopsis ovata*? Harmful Algae 10, 165–172.
801 https://doi.org/10.1016/j.hal.2010.09.002
802 Hallegraeff, G.M., 2010. Ocean climate change, phytoplankton community responses, and
803 harmful algal blooms: a formidable predictive challenge. J. Phycol. 46, 220–235.
804 https://doi.org/10.1111/j.1529-8817.2010.00815.x
805 Hallegraeff, G.M., Anderson, D.M., Belin, C., Bottein, M.-Y.D., Bresnan, E., Chinain, M.,
806 Enevoldsen, H., Iwataki, M., Karlson, B., McKenzie, C.H., Sunesen, I., Pitcher, G.C.,
807 Provoost, P., Richardson, A., Schweibold, L., Tester, P.A., Trainer, V.L., Yñiguez,
808 A.T., Zingone, A., 2021. Perceived global increase in algal blooms is attributable to
809 intensified monitoring and emerging bloom impacts. Commun. Earth Environ. 2, 117.
810 https://doi.org/10.1038/s43247-021-00178-8
811 Hamilton, G., McVinish, R., Mengersen, K., 2009. Bayesian model averaging for harmful
812 algal bloom prediction. Ecol. Appl. 19, 1805–1814. https://doi.org/10.1890/08-1843.1
813 Heisler, J., Glibert, P.M., Burkholder, J.M., Anderson, D.M., Cochlan, W., Dennison, W.C.,
814 Dortch, Q., Gobler, C.J., Heil, C.A., Humphries, E., Lewitus, A., Magnien, R.,
815 Marshall, H.G., Sellner, K., Stockwell, D.A., Stoecker, D.K., Suddleson, M., 2008.
816 Eutrophication and harmful algal blooms: A scientific consensus. Harmful Algae 8, 3–
817 13. https://doi.org/10.1016/j.hal.2008.08.006
818 Hoppenrath, M., Murray, S.A., Chomérat, N., Horiguchi, T., 2014. Marine benthic
819 dinoflagellates: unveiling their worldwide biodiversity, Kleine Senckenberg-Reihe. E.
820 Schweizerbart'sche Verlagsbuchhandlung, Stuttgart.
821 Illoul, H., Hernández, F.R., Vila, M., Adjas, N., younes, A.A., Bournissa, M., Koroghli, A.,
822 Marouf, N., Rabia, S., Ameur, F.L.K., 2012. The Genus *Ostreopsis* along the Algerian
823 Coastal Waters (SW Mediterranean Sea) Associated with a Human Respiratory
824 Intoxication Episode. Cryptogam. Algol. 33, 209–216.
825 https://doi.org/10.7872/crya.v33.iss2.2011.209
826 Jauzein, C., Açaf, L., Accoroni, S., Asnaghi, V., Fricke, A., Hachani, M.A., abboud-Abi Saab,
827 M., Chiantore, M., Mangialajo, L., Totti, C., Zaghmouri, I., Lemée, R., 2018.
828 Optimization of sampling, cell collection and counting for the monitoring of benthic
829 harmful algal blooms: Application to *Ostreopsis* spp. blooms in the Mediterranean
830 Sea. Ecol. Indic. 91, 116–127. https://doi.org/10.1016/j.ecolind.2018.03.089
831 Jauzein, C., Couet, D., Blasco, T., Lemée, R., 2017. Uptake of dissolved inorganic and
832 organic nitrogen by the benthic toxic dinoflagellate *Ostreopsis* cf. *ovata*. Harmful
833 Algae 65, 9–18. https://doi.org/10.1016/j.hal.2017.04.005

834 Kibler, S.R., Tester, P.A., Kunkel, K.E., Moore, S.K., Litaker, R.W., 2015. Effects of ocean
835 warming on growth and distribution of dinoflagellates associated with ciguatera fish
836 poisoning in the Caribbean. Ecol. Model. 316, 194–210.
837 https://doi.org/10.1016/j.ecolmodel.2015.08.020
838 Lau, W.L.S., Law, I.K., Liow, G.R., Hii, K.S., Usup, G., Lim, P.T., Leaw, C.P., 2017. Life-
839 history stages of natural bloom populations and the bloom dynamics of a tropical
840 Asian ribotype of *Alexandrium minutum*. Harmful Algae 70, 52–63.
841 https://doi.org/10.1016/j.hal.2017.10.006
842 Lee, B., Park, M.G., 2018. Genetic Analyses of the rbcL and psaA Genes From Single Cells
843 Demonstrate a Rhodophyte Origin of the Prey in the Toxic Benthic Dinoflagellate
844 *Ostreopsis*. Front. Mar. Sci. 5, 217. https://doi.org/10.3389/fmars.2018.00217
845 Maguire, J., Cusack, C., Ruiz-Villarreal, M., Silke, J., McElligott, D., Davidson, K., 2016.
846 Applied simulations and integrated modelling for the understanding of toxic and
847 harmful algal blooms (ASIMUTH): Integrated HAB forecast systems for Europe's
848 Atlantic Arc. Harmful Algae 53, 160–166. https://doi.org/10.1016/j.hal.2015.11.006
849 Mangialajo, L., Bertolotto, R., Cattaneo-Vietti, R., Chiantore, M., Grillo, C., Lemee, R.,
850 Melchiorre, N., Moretto, P., Povero, P., Ruggieri, N., 2008. The toxic benthic
851 dinoflagellate *Ostreopsis ovata*: Quantification of proliferation along the coastline of
852 Genoa, Italy. Mar. Pollut. Bull. 56, 1209–1214.
853 https://doi.org/10.1016/j.marpolbul.2008.02.028
854 Mangialajo, L., Ganzin, N., Accoroni, S., Asnaghi, V., Blanfuné, A., Cabrini, M., Cattaneo-
855 Vietti, R., Chavanon, F., Chiantore, M., Cohu, S., Costa, E., Fornasaro, D., Grossel,
856 H., Marco-Miralles, F., Masó, M., Reñé, A., Rossi, A.M., Sala, M.M., Thibaut, T.,
857 Totti, C., Vila, M., Lemée, R., 2011. Trends in *Ostreopsis* proliferation along the
858 Northern Mediterranean coasts. Toxicon 57, 408–420.
859 https://doi.org/10.1016/j.toxicon.2010.11.019
860 Meroni, L., Chiantore, M., Petrillo, M., Asnaghi, V., 2018. Habitat effects on *Ostreopsis* cf.
861 *ovata* bloom dynamics. Harmful Algae 80, 64–71.
862 https://doi.org/10.1016/j.hal.2018.09.006
863 Moita, M.T., Pazos, Y., Rocha, C., Nolasco, R., Oliveira, P.B., 2016. Toward predicting
864 *Dinophysis* blooms off NW Iberia: A decade of events. Harmful Algae 53, 17–32.
865 https://doi.org/10.1016/j.hal.2015.12.002
866 Monti, M., Minocci, M., Beran, A., Iveša, L., 2007. First record of *Ostreopsis* cfr. *ovata* on
867 macroalgae in the Northern Adriatic Sea. Mar. Pollut. Bull. 54, 598–601.
868 https://doi.org/10.1016/j.marpolbul.2007.01.013
869 Montresor, M., Lewis, J., 2006. Phases, stages and shifts in the life cycles of marine
870 phytoplankton. DV Subba-Rao Ed Algal Cult. Analog. Blooms Appl. Sci. Publ.
871 Enfield USA 2006 91–129.
872 Moore, S.K., Bill, B.D., Hay, L.R., Emenegger, J., Eldred, K.C., Greengrove, C.L., Masura,
873 J.E., Anderson, D.M., 2015. Factors regulating excystment of *Alexandrium* in Puget
874 Sound, WA, USA. Harmful Algae 43, 103–110.
875 https://doi.org/10.1016/j.hal.2015.01.005
876 Moore, S.K., Trainer, V.L., Mantua, N.J., Parker, M.S., Laws, E.A., Backer, L.C., Fleming,
877 L.E., 2008. Impacts of climate variability and future climate change on harmful algal
878 blooms and human health. Environ. Health 7, S4. https://doi.org/10.1186/1476-069X-
879 7-S2-S4
880 Nakada, M., Hatayama, Y., Ishikawa, A., Ajisaka, T., Sawayama, S., Imai, I., 2018. Seasonal
881 distribution of *Gambierdiscus* spp. in Wakasa Bay, the Sea of Japan, and antagonistic
882 relationships with epiphytic pennate diatoms. Harmful Algae 76, 58–65.
883 https://doi.org/10.1016/j.hal.2018.05.002

Ní Rathaille, A., Raine, R., 2011. Seasonality in the excystment of *Alexandrium minutum* and *Alexandrium tamarense* in Irish coastal waters. Harmful Algae 10, 629–635. https://doi.org/10.1016/j.hal.2011.04.015

Ninčević Gladan, Ž., Arapov, J., Casabianca, S., Penna, A., Honsell, G., Brovedani, V., Pelin, M., Tartaglione, L., Sosa, S., Dell'Aversano, C., Tubaro, A., Žuljević, A., Grbec, B., Čavar, M., Bužančić, M., Bakrač, A., Skejić, S., 2019. Massive Occurrence of the Harmful Benthic Dinoflagellate *Ostreopsis* cf. *ovata* in the Eastern Adriatic Sea. Toxins 11, 300. https://doi.org/10.3390/toxins11050300

Parsons, M.L., Aligizaki, K., Bottein, M.-Y.D., Fraga, S., Morton, S.L., Penna, A., Rhodes, L., 2012. *Gambierdiscus* and *Ostreopsis*: Reassessment of the state of knowledge of their taxonomy, geography, ecophysiology, and toxicology. Harmful Algae 14, 107–129. https://doi.org/10.1016/j.hal.2011.10.017

Pezzolesi, L., Guerrini, F., Ciminiello, P., Dell'Aversano, C., Iacovo, E.D., Fattorusso, E., Forino, M., Tartaglione, L., Pistocchi, R., 2012. Influence of temperature and salinity on *Ostreopsis* cf. *ovata* growth and evaluation of toxin content through HR LC-MS and biological assays. Water Res. 46, 82–92. https://doi.org/10.1016/j.watres.2011.10.029

Pfannkuchen, M., Godrijan, J., Marić Pfannkuchen, D., Iveša, L., Kružić, P., Ciminiello, P., Dell'Aversano, C., Dello Iacovo, E., Fattorusso, E., Forino, M., Tartaglione, L., Godrijan, M., 2012. Toxin-Producing *Ostreopsis* cf. *ovata* are Likely to Bloom Undetected along Coastal Areas. Environ. Sci. Technol. 46, 5574–5582. https://doi.org/10.1021/es300189h

Pistocchi, R., Pezzolesi, L., Guerrini, F., Vanucci, S., Dell'Aversano, C., Fattorusso, E., 2011. A review on the effects of environmental conditions on growth and toxin production of *Ostreopsis ovata*. Toxicon 57, 421–428. https://doi.org/10.1016/j.toxicon.2010.09.013

R Core Team, 2019. R: A language and environment for statistical computing. R Found. Stat. Comput. Vienna Austria.

Rhodes, L., 2011. World-wide occurrence of the toxic dinoflagellate genus *Ostreopsis* Schmidt. Toxicon 57, 400–407. https://doi.org/10.1016/j.toxicon.2010.05.010

Rigosi, A., Hanson, P., Hamilton, D.P., Hipsey, M., Rusak, J.A., Bois, J., Sparber, K., Chorus, I., Watkinson, A.J., Qin, B., Kim, B., Brookes, J.D., 2015. Determining the probability of cyanobacterial blooms: the application of Bayesian networks in multiple lake systems. Ecol. Appl. 25, 186–199. https://doi.org/10.1890/13-1677.1

Ruiz-Villarreal, M., García-García, L.M., Cobas, M., Díaz, P.A., Reguera, B., 2016. Modelling the hydrodynamic conditions associated with *Dinophysis* blooms in Galicia (NW Spain). Harmful Algae 53, 40–52. https://doi.org/10.1016/j.hal.2015.12.003

Sansoni, G., Borghini, B., Camici, G., Casotti, M., Righini, P., Rustighi, C., 2003. Fioriture algali di *Ostreopsis ovata* (Gonyaulacales: Dinophyceae): un problema emergente. Biol. Ambiantale 17, 17–23.

Scalco, E., Brunet, C., Marino, F., Rossi, R., Soprano, V., Zingone, A., Montresor, M., 2012. Growth and toxicity responses of Mediterranean *Ostreopsis* cf. *ovata* to seasonal irradiance and temperature conditions. Harmful Algae 17, 25–34. https://doi.org/10.1016/j.hal.2012.02.008

Shears, N.T., Ross, P.M., 2009. Blooms of benthic dinoflagellates of the genus *Ostreopsis*; an increasing and ecologically important phenomenon on temperate reefs in New Zealand and worldwide. Harmful Algae 8, 916–925. https://doi.org/10.1016/j.hal.2009.05.003

Tawong, W., Yoshimatsu, T., Yamaguchi, H., Adachi, M., 2015. Effects of temperature, salinity and their interaction on growth of benthic dinoflagellates *Ostreopsis* spp. from Thailand. Harmful Algae 44, 37–45. https://doi.org/10.1016/j.hal.2015.02.011

Taylor, F.J.R., 1979. The description of the benthic dinoflagellate associated with maitotoxin and ciguatoxin, including observations on Hawaiian material. DL Taylor HH Seliger Eds Toxic Dinoflag. Blooms Elsevier Sci. NY 71–77.

Tester, P.A., Litaker, R.W., Berdalet, E., 2020. Climate change and harmful benthic microalgae. Harmful Algae 91, 101655. https://doi.org/10.1016/j.hal.2019.101655

Tichadou, L., Glaizal, M., Armengaud, A., Grossel, H., Lemée, R., Kantin, R., Lasalle, J.-L., Drouet, G., Rambaud, L., Malfait, P., de Haro, L., 2010. Health impact of unicellular algae of the *Ostreopsis* genus blooms in the Mediterranean Sea: experience of the French Mediterranean coast surveillance network from 2006 to 2009. Clin. Toxicol. 48, 839–844. https://doi.org/10.3109/15563650.2010.513687

Totti, C., Accoroni, S., Cerino, F., Cucchiari, E., Romagnoli, T., 2010. *Ostreopsis ovata* bloom along the Conero Riviera (northern Adriatic Sea): Relationships with environmental conditions and substrata. Harmful Algae 9, 233–239. https://doi.org/10.1016/j.hal.2009.10.006

Tubaro, A., Durando, P., Del Favero, G., Ansaldi, F., Icardi, G., Deeds, J.R., Sosa, S., 2011. Case definitions for human poisonings postulated to palytoxins exposure. Toxicon 57, 478–495. https://doi.org/10.1016/j.toxicon.2011.01.005

Utermöhl, H., 1958. Zur Vervollkommnung der quantitativen Phytoplankton-Methodik: Mit 1 Tabelle und 15 abbildungen im Text und auf 1 Tafel. SIL Commun. 1953-1996 9, 1–38. https://doi.org/10.1080/05384680.1958.11904091

Van Dolah, F.M., 2000. Marine algal toxins: origins, health effects, and their increased occurrence. Environ. Health Perspect. 108, 133–141. https://doi.org/10.1289/ehp.00108s1133

Vila, M., Abós-Herràndiz, R., Isern-Fontanet, J., Àlvarez, J., Berdalet, E., 2016. Establishing the link between *Ostreopsis* cf.*ovata* blooms and human health impacts using ecology and epidemiology. Sci. Mar. 80, 107–115. https://doi.org/10.3989/scimar.04395.08A

Vila, M., Garcés, E., Masó, M., 2001. Potentially toxic epiphytic dinoflagellate assemblages on macroalgae in the NW Mediterranean. Aquat. Microb. Ecol. 26, 51–60. https://doi.org/10.3354/ame026051

Vila, M., Masó, M., Sampedro, N., Illoul, H., Arin, L., Garcés, E., Giacobbe, M.G., Alvarez, J., Camp, J., 2008. The genus *Ostreopsis* in the recreational waters along the Catalan Coast and Balearic Islands (NW Mediterranean Sea): are they the origin of human respiratory difficulties? Proc. 12th Int. Conf. Harmful Algae 2008 334–336.

Wells, M.L., Karlson, B., 2018. Harmful Algal Blooms in a Changing Ocean, in: Glibert, P.M., Berdalet, E., Burford, M.A., Pitcher, G.C., Zhou, M. (Eds.), Global Ecology and Oceanography of Harmful Algal Blooms. Springer International Publishing, Cham, pp. 77–90. https://doi.org/10.1007/978-3-319-70069-4_5

Wells, M.L., Karlson, B., Wulff, A., Kudela, R., Trick, C., Asnaghi, V., Berdalet, E., Cochlan, W., Davidson, K., De Rijcke, M., Dutkiewicz, S., Hallegraeff, G., Flynn, K.J., Legrand, C., Paerl, H., Silke, J., Suikkanen, S., Thompson, P., Trainer, V.L., 2020. Future HAB science: Directions and challenges in a changing climate. Harmful Algae 91, 101632. https://doi.org/10.1016/j.hal.2019.101632

Wells, M.L., Trainer, V.L., Smayda, T.J., Karlson, B.S.O., Trick, C.G., Kudela, R.M., Ishikawa, A., Bernard, S., Wulff, A., Anderson, D.M., Cochlan, W.P., 2015. Harmful algal blooms and climate change: Learning from the past and present to forecast the future. Harmful Algae 49, 68–93. https://doi.org/10.1016/j.hal.2015.07.009

Wood, A.M., Everroad, R.C., Wingard, L.M., 2005. Measuring growth rates in microalgal cultures. Algal Cult. Tech. 269–288.

Fig. 1: Map of the sampling sites (1 to 5) in Larvotto beach, Monaco. The inside top-left corner shows the NW Mediterranean Sea map, with the location of Monaco state.

Fig. 2: Temporal variations of benthic *Ostreopsis* cf. *ovata* abundances (bars, left Y-axis) and sea surface temperatures (dotted line, right Y-axis) in summer (from June 10 to September 2, X axis) in Larvotto (Monaco) from 2007 to 2019.

Fig. 3: Correlation between benthic and planktonic cell abundances of *Ostreopsis* cf. *ovata* in Larvotto beach (Monaco) considering the 13-year data set.

Fig. 4: Biplot representation of environmental parameters and individuals on the first two axis of the Principal Component Analysis (PCA). Mean spring values (April-May-June) of variables used to create the factorial space (SST, Salinity, Rainfall, South-North and West-East Wind intensity and both nitrate and nitrite surface concentrations) are represented by solid arrows. The grey/black gradient of the arrows represents the Cos^2 of the variables. Variables associated with phenological features (Bloom Starting Day, Bloom Duration, Maximum Intensity and Maximum Growth Rate) were added as supplementary variables to the analysis and represented by dashed red arrows.

Fig. 5: Variation of positive net growth rates with sea surface temperatures. Circled dots represent the highest positive growth rate value for each year of the survey. Black line is the loess regression model with 95% confident interval in grey.

Fig. 6: Weekly cumulative sum of SST anomalies in Point B (Villefranche-sur-Mer) corresponding to each year of survey. The spring season (April, May and June) is highlighted in grey.

Fig 7: Correlation between bloom starting day and cumulative sum of SST anomalies: (A) Example of cumulative sum of SST anomalies averaged for June compared to bloom starting days for each year of the survey (2007 excluded). (B) Strength of correlations represented by the Spearman r_s^2 for each averaged month and spring season (*: $p < 0.05$; **: $p < 0.01$).

Table 1: Environmental parameters collected over the spring (April-May-June) period. Bold values represent the mean (± Standard Deviation) and values in brackets represent the range between minimal and maximal values recorded.

Table 2: Correlation and Cos^2 values of active and illustrative variables for the first three dimensions of the PCA analysis.

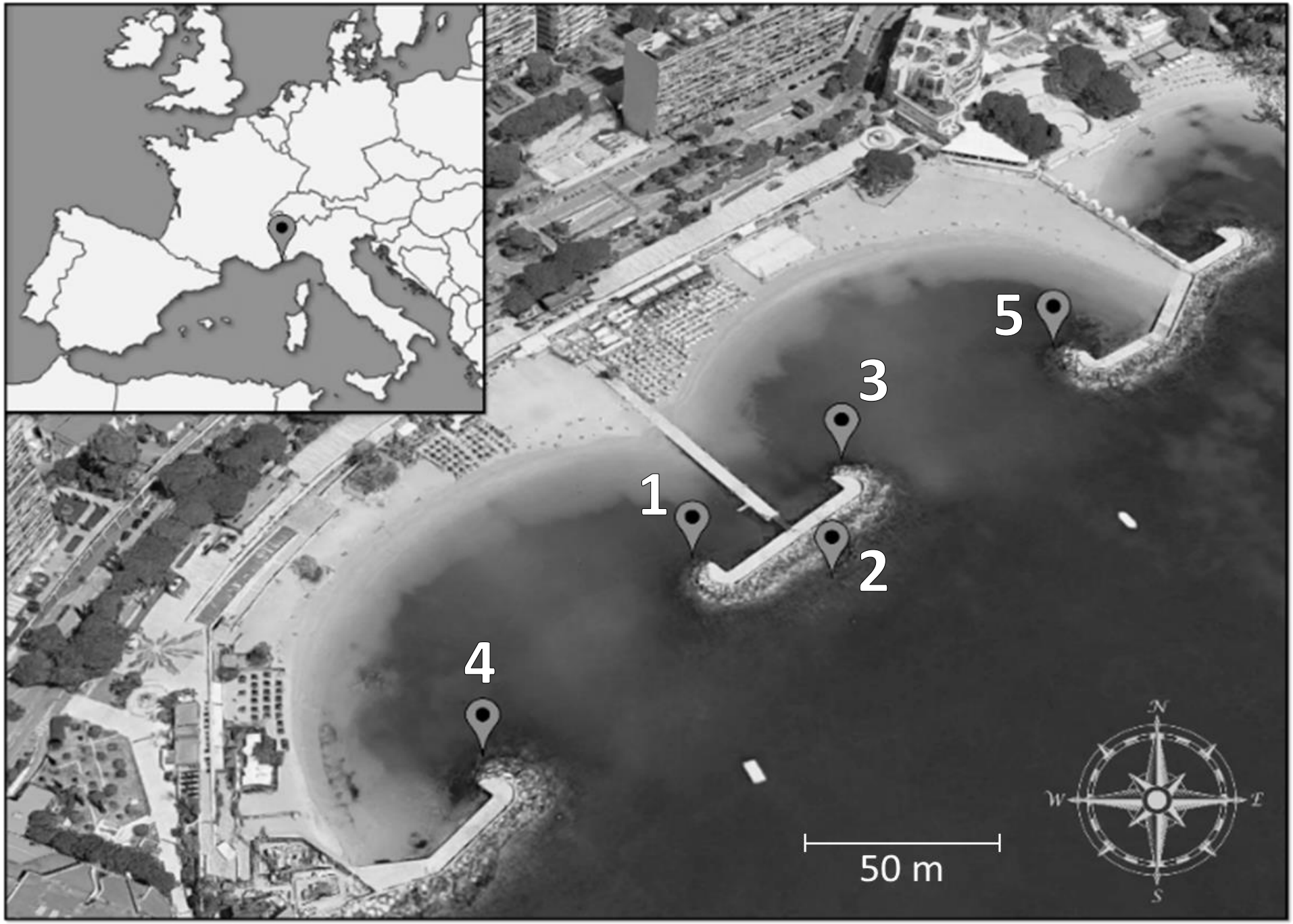
5
3
1
2
4
50 m
N
W
E
S

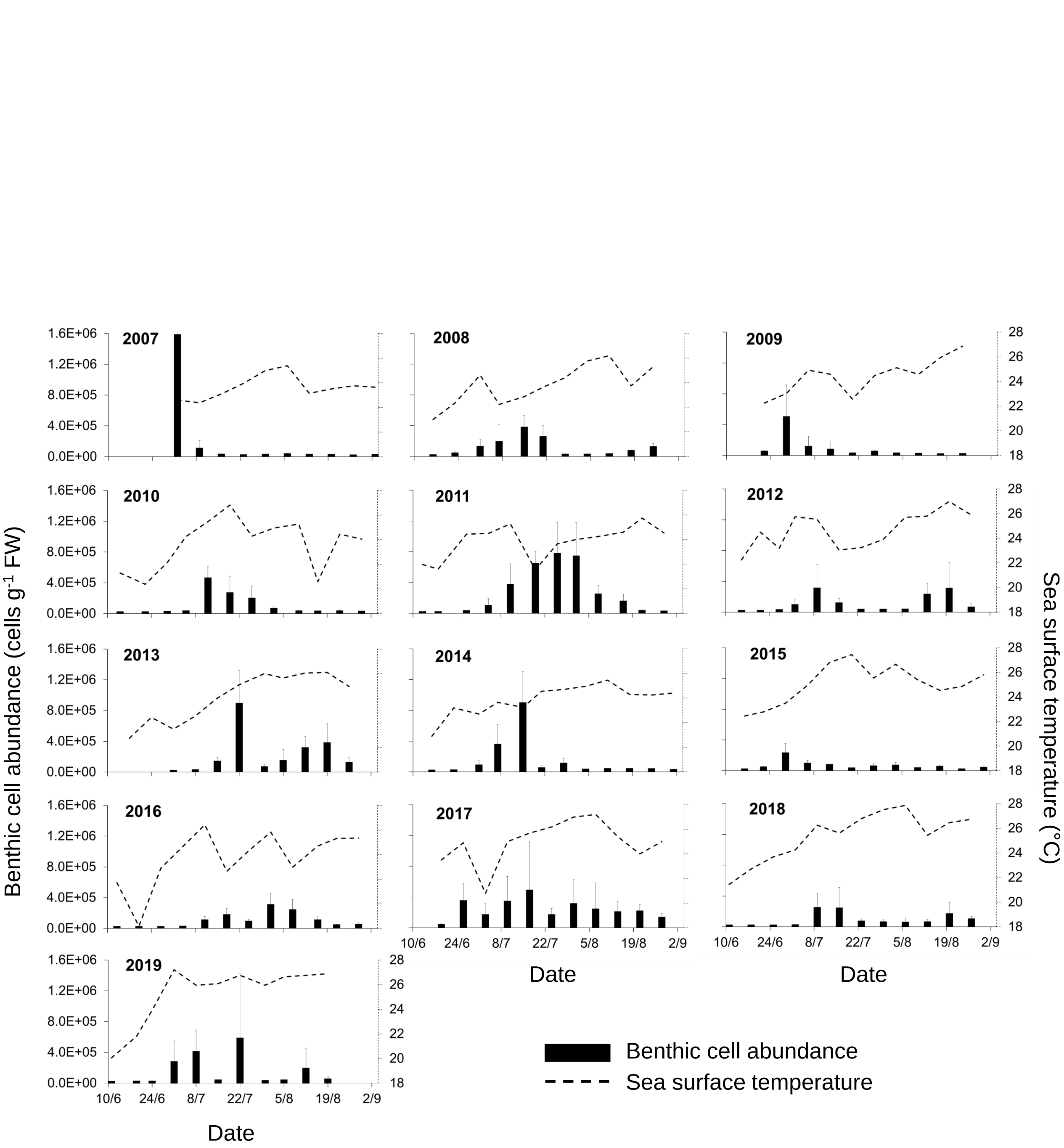
2007
2008
2009
2010
2011
2012
2013
2014
2015
2016
2017
2018
2019
1.6E+06
1.2E+06
8.0E+05
4.0E+05
0.0E+00
28
26
24
22
20
18
10/6
24/6
8/7
22/7
5/8
19/8
2/9
Benthic cell abundance (cells g-1 FW)
Sea surface temperature (°C)
Date
Benthic cell abundance
Sea surface temperature

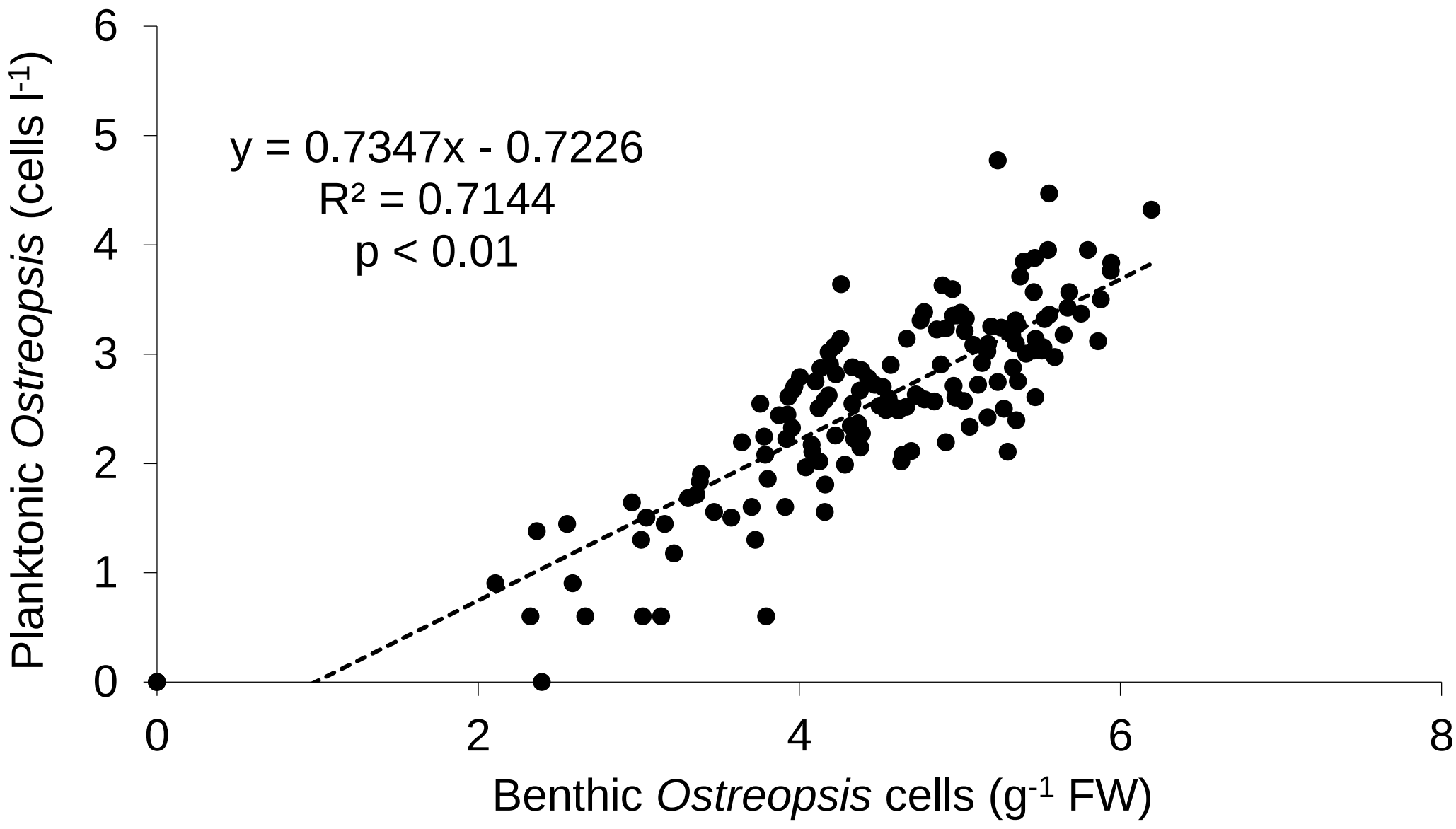
y = 0.7347x - 0.7226
R² = 0.7144
p < 0.01
Planktonic Ostreopsis (cells l-1)
Benthic Ostreopsis cells (g-1 FW)
0
1
2
3
4
5
6
0
2
4
6
8

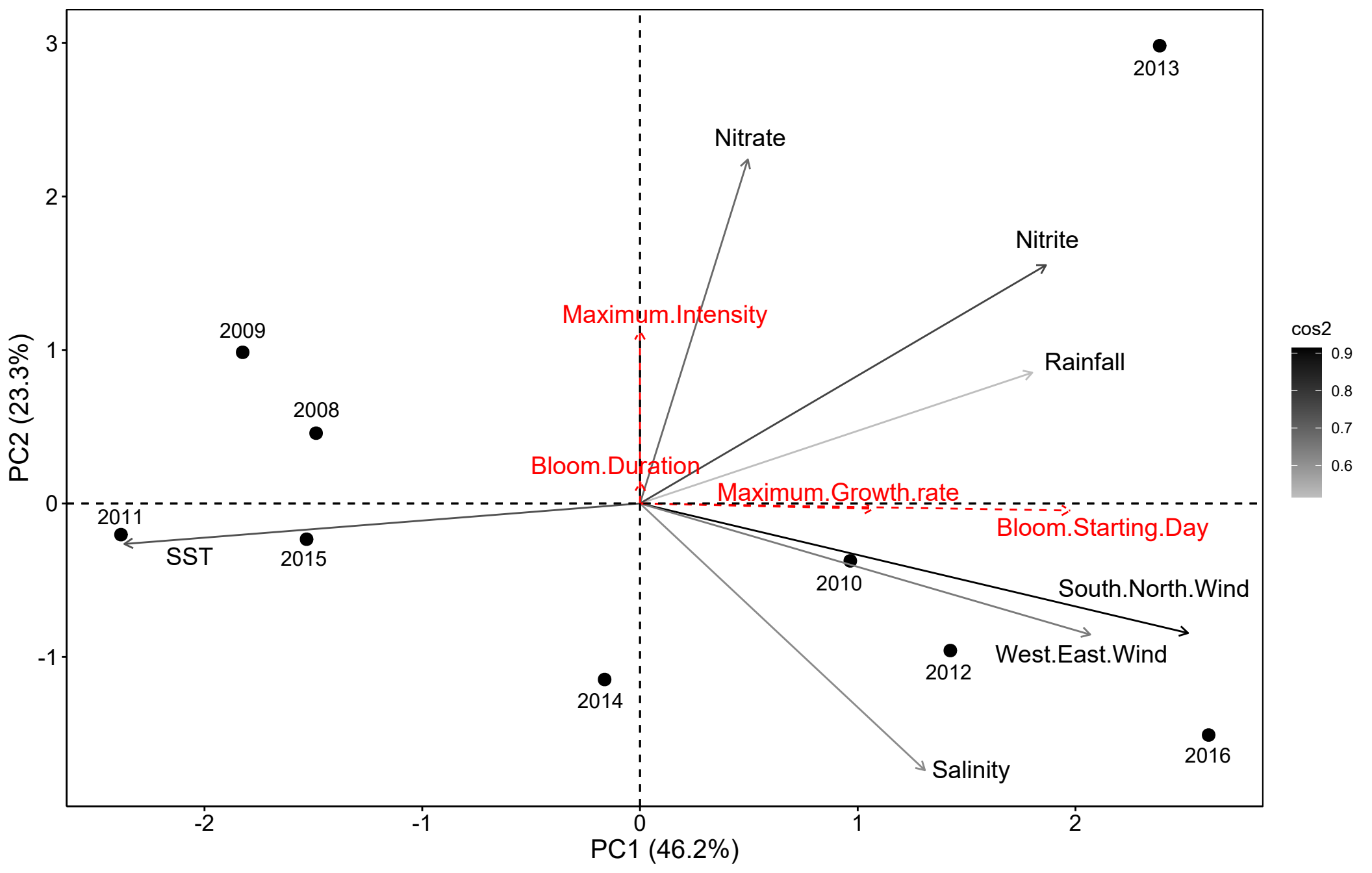
2013
Nitrate
Nitrite
Maximum.Intensity
2009
Rainfall
2008
Bloom.Duration
Maximum.Growth.rate
2011
Bloom.Starting.Day
SST
2015
2010
South.North.Wind
West.East.Wind
2012
2014
2016
Salinity
PC2 (23.3%)
PC1 (46.2%)
cos2
0.9
0.8
0.7
0.6
3
2
1
0
-1
-2
-1
0
1
2

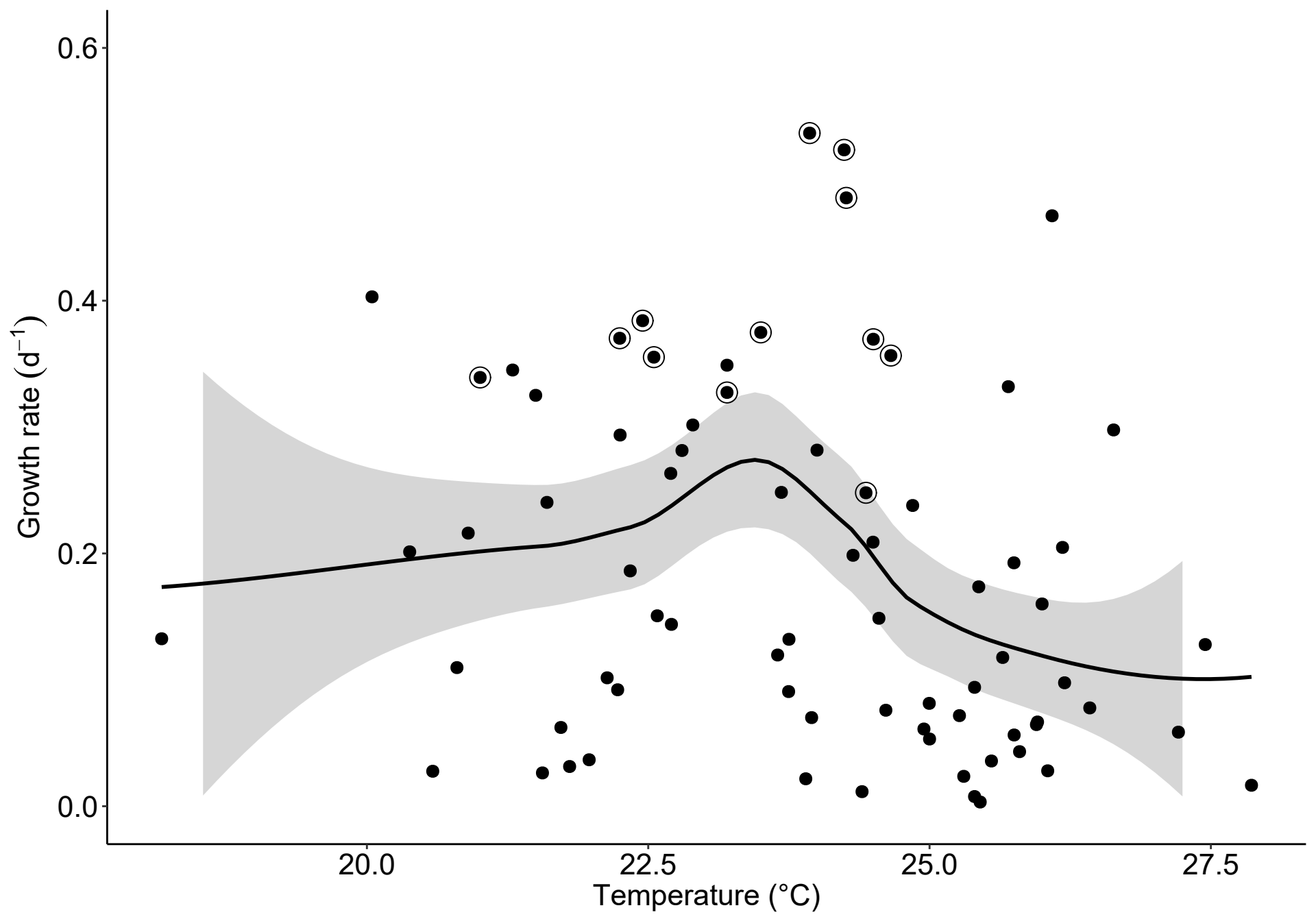
0.6
0.4
0.2
0.0
Growth rate (d^{-1})
20.0
22.5
25.0
27.5
Temperature (°C)

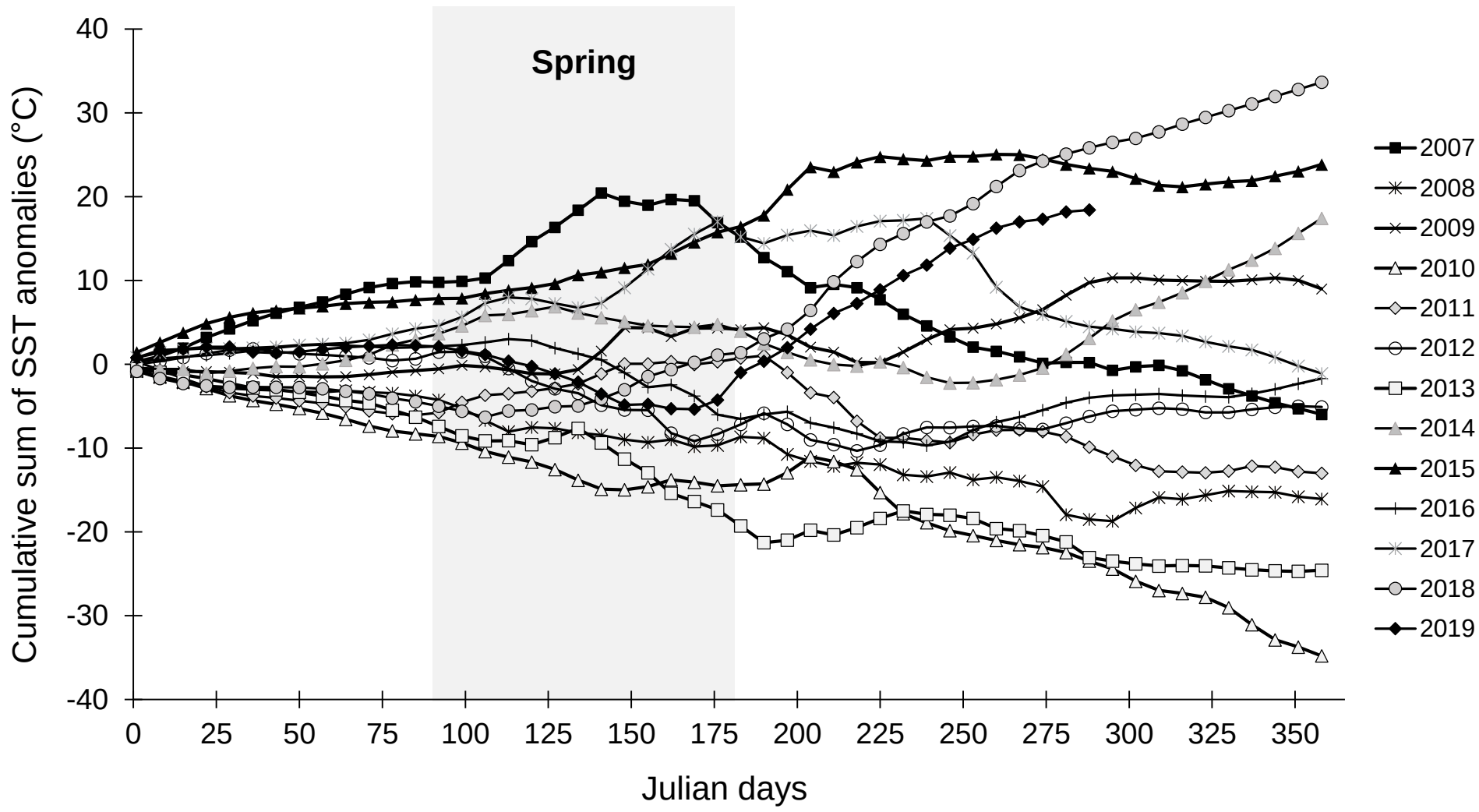
Spring
Cumulative sum of SST anomalies (°C)
Julian days
40
30
20
10
0
-10
-20
-30
-40
0
25
50
75
100
125
150
175
200
225
250
275
300
325
350
2007
2008
2009
2010
2011
2012
2013
2014
2015
2016
2017
2018
2019

A

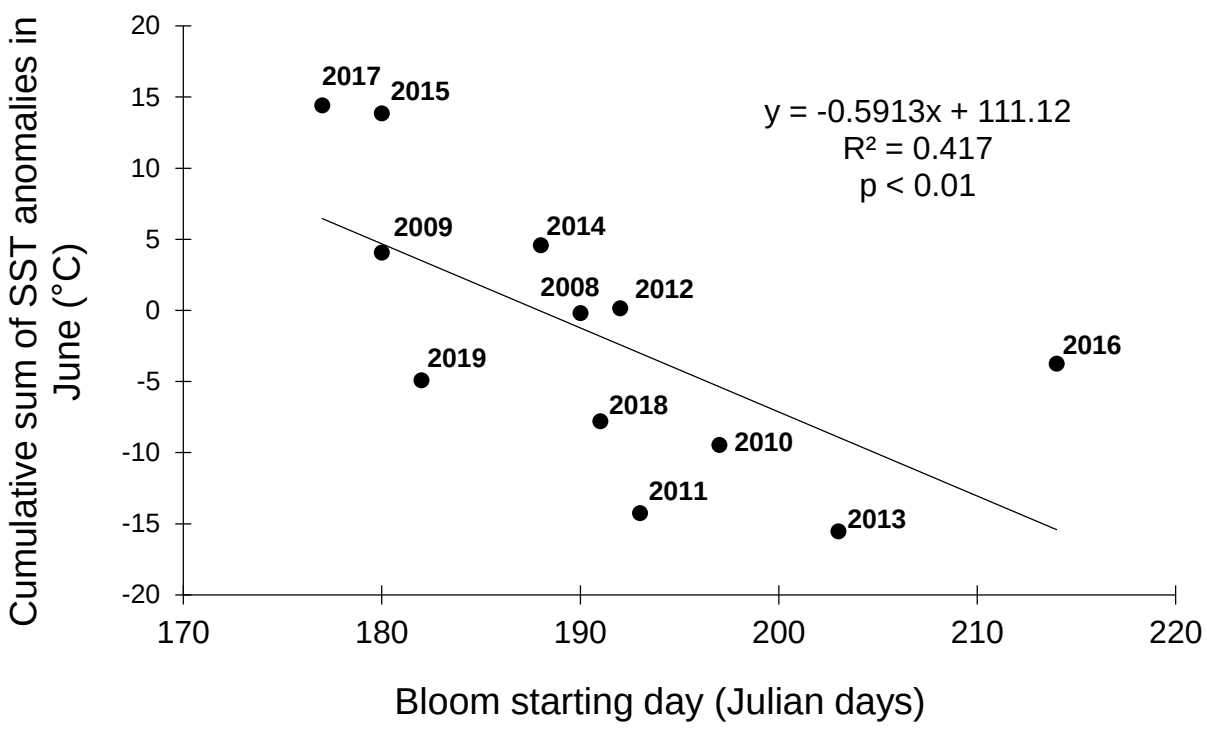
y = -0.5913x + 111.12
R² = 0.417
p < 0.01
2017
2015
2009
2014
2008
2012
2016
2019
2018
2010
2011
2013
Cumulative sum of SST anomalies in June (°C)
Bloom starting day (Julian days)

B

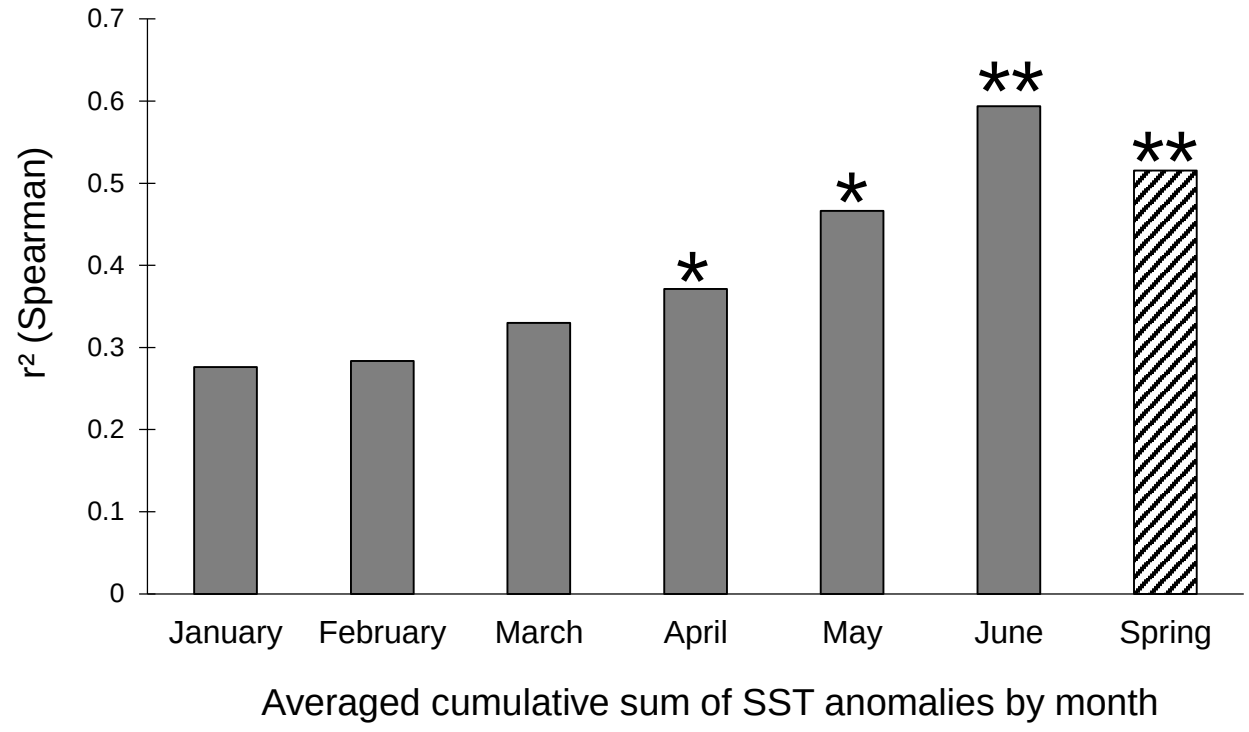
r² (Spearman)
January
February
March
April
May
June
Spring
Averaged cumulative sum of SST anomalies by month

Year	SST (°C)	Salinity	Rainfall (ml)	Wind speed (m/s)	Nitrates ($\mu mol.l^{-1}$)	Nitrites ($\mu mol.l^{-1}$)
2007	**18.8** ±2.3 (14.1 - 21.7)	**37.7** ±0.2 (37.3 - 38.1)	**0.2** ±1.6 (0 - 15.0)	**3.1** ±1.7 (1.4 - 8.5)	**0.6** ±0.8 (0.2 - 2.7)	**0.1** ±0.1 (0 - 0.5)
2008	**18.0** ±3.6 (13.7 - 25.2)	**37.7** ±0.3 (37 - 38.1)	**0.2** ±0.6 (0 - 4.0)	**3.4** ±2.0 (1.2 - 10.2)	**0.2** ±0.1 (0.1 - 0.3)	**0.1** ±0.0 (0.1 - 0.2)
2009	**18.5** ±3.4 (14.0 - 23.2)	**37.5** ±0.3 (36.8 - 37.9)	**0.2** ±0.7 (0 - 4.4)	**3.3** ±1.8 (1.2 - 11.6)	**0.6** ±0.4 (0.1 - 1.4)	**0.0** ±0.0 (0 - 0.1)
2010	**17.7** ±3.4 (13.9 - 23.7)	**37.6** ±0.2 (37.3 - 37.8)	**0.6** ±2.3 (0 - 16.0)	**3.1** ±1.9 (0.8 - 14.3)	**0.2** ±0.2 (0 - 0.6)	**0.1** ±0.1 (0 - 0.2)
2011	**18.4** ±3.0 (13.6 - 24.2)	**37.7** ±0.3 (37.1 - 37.9)	**0.5** ±1.6 (0 - 9.6)	**2.8** ±1.5 (1.1 - 11.4)	**0.3** ±0.3 (0.1 - 1.0)	**0.0** ±0.0 (0 - 0.1)
2012	**18.1** ±3.8 (13.8 - 25.6)	**38.0** ±0.1 (37.6 - 38.2)	**1.7** ±4.9 (0 - 24.4)	**3.3** ±2 (0.9 - 9.6)	**0.2** ±0.3 (0 - 1.0)	**0.1** ±0.0 (0 - 0.1)
2013	**17.5** ±2.8 (13.1 - 22.0)	**37.6** ±0.3 (37.1 - 38.0)	**1.8** ±5.1 (0 - 34.2)	**3.3** ±1.8 (0.9 - 10.6)	**0.7** ±0.4 (0.2 - 1.5)	**0.1** ±0.2 (0 - 0.6)
2014	**18.0** ±2.5 (14.8 - 23.1)	**37.7** ±0.2 (37.3 - 37.8)	**0.5** ±1.7 (0 - 14.4)	**3.1** ±1.8 (0.7 - 11.3)	**0.2** ±0.1 (0.1 - 0.4)	**0.0** ±0.0 (0 - 0.1)
2015	**18.8** ±3.4 (14.3 - 24.3)	**37.8** ±0.1 (37.5 - 38)	**0.8** ±3.4 (0 - 24.6)	**2.8** ±1.5 (0.5 - 9.2)	**0.3** ±0.2 (0.1 - 1.0)	**0.0** ±0.0 (0 - 0.1)
2016	**17.5** ±2.6 (14.1 - 22.8)	**38.0** ±0.1 (37.9 - 38.1)	**0.7** ±2.4 (0 - 20.4)	**3.3** ±1.7 (1.4 - 8.7)	**0.4** ±0.2 (0.1 - 0.7)	**0.1** ±0.1 (0 - 0.3)
2017	**18.8** ±3.6 (14.4 - 24.5)	**38.0** ±0.1 (37.9 - 38.1)	ND	ND	**0.4** ±0.1 (0.2 - 0.8)	**0.0** ±0.0 (0 - 0.1)

2018	**18.8** ±3.7 (13.5 - 24.2)	**37.7** ±0.3 (36.9 - 38.1)	ND	ND	ND	ND
2019	**18.1** ±4.0 (14.0 - 27.2)	ND	ND	ND	ND	ND

Variables		Dimension 1		Dimension 2		Dimension 3	
		Correlation	Cos^2	Correlation	Cos^2	Correlation	Cos^2
Active	SST	-0.85	0.73	-0.10	0.01	0.35	0.13
	Rainfall	0.65	0.42	0.31	0.09	0.63	0.40
	South-North Wind	0.91	0.82	-0.30	0.09	-0.25	0.06
	West-East Wind	0.74	0.55	-0.31	0.09	-0.19	0.04
	Salinity	0.47	0.22	-0.63	0.39	0.53	0.28
	Nitrate	0.18	0.03	0.81	0.65	0.04	0.00
	Nitrite	0.67	0.45	0.56	0.31	0.01	0.00
Illustrative	Bloom starting day	0.71	0.51	-0.02	0.00	-0.12	0.01
	Bloom duration	0.00	0.00	0.05	0.00	0.32	0.10
	Maximum intensity	0.00	0.00	0.40	0.16	-0.28	0.08
	Maximum growth rate	0.39	0.15	-0.01	0.00	-0.30	0.09